NASA TECHNICAL NOTE

POWER SPECTRAL MEASUREMENT OF ATMOSPHERIC TURBULENCE IN SEVERE STORMS AND CUMULUS CLOUDS

by Richard H. Rhyne and Roy Steiner

Langley Research Center
Langley Station, Hampton, Va.

POWER SPECTRAL MEASUREMENT OF ATMOSPHERIC TURBULENCE

IN SEVERE STORMS AND CUMULUS CLOUDS

By Richard H. Rhyne and Roy Steiner

Langley Research Center
Langley Station, Hampton, Va.

NATIONAL AERONAUTICS AND SPACE ADMINISTRATION

POWER SPECTRAL MEASUREMENT OF ATMOSPHERIC TURBULENCE

IN SEVERE STORMS AND CUMULUS CLOUDS

By Richard H. Rhyne and Roy Steiner
Langley Research Center

SUMMARY

The report summarizes power spectral data of atmospheric turbulence obtained by the NASA from recent flights in severe storms and cumulus clouds. For completeness, previously published spectra are included. These spectra are similar in shape to those obtained in clear air at altitudes below 5,000 feet. The power varies inversely with frequency to the five-thirds power.

As an indication of the turbulence intensity, values of root-mean-square gust velocity determined from the measured spectra ranged from approximately 6 to 16 ft/sec for the severe-storm traverses and from about 3 to 9 ft/sec for the cumulus-cloud traverses. Storm turbulence was found to be homogeneous and stationary, isotropic, and Gaussian to a degree sufficient for many practical applications. Values of L, a scale parameter required in the analytical representation of the spectra, were obtained for five storm traverses. The values obtained range from approximately 2,700 to 5,600 feet. Additional investigation. is needed to more completely define the factors on which L itself depends.

INTRODUCTION

During the past decade more and more interest has been focused on the description of atmospheric turbulence as a continuous process and on the use of power spectral techniques in the analysis of turbulence and the associated dynamic load and motion response of airplanes. Today, airplane designers are turning to spectral techniques to check their design, although power spectral methods have not as yet been officially incorporated into design requirements as such. For use in such design studies, experimentally determined spectra of atmospheric turbulence in clear air at relatively low altitudes (below 5,000 feet) have been collected by the National Aeronautics and Space Administration (refs. 1, 2, and 3) and by others (refs. 4 and 5).

The present report summarizes power spectral data obtained by the NASA from flight tests in severe storms and cumulus clouds. ("Severe storms" are defined herein as convective storms with sufficient energy to build through the tropopause to an altitude of at least 40,000 feet and are usually thunderstorms.) Turbulence, when associated with the more severe convective activity, can produce extremely severe loads, in fact, the highest loads which transport-type airplanes may ever experience during normal operations. The severe-storm

penetrations were made in the vicinity of Tinker Air Force Base, Oklahoma, in conjunction with the National Severe Storms Project (refs. 6 and 7), and consist of 11 different penetrations (three separate storms) at altitudes ranging from 25,000 to 40,000 feet. The cumulus-cloud data were obtained in the vicinity of Langley Air Force Base, Virginia, from nine traverses which ranged in altitude from 7,000 to 15,000 feet. Initial samples of the data obtained from both of these investigations have been published in references 8 and 9.

The data are generally presented in the form of power spectra of the vertical and lateral components, and where available, the longitudinal component of atmospheric turbulence. Estimates are made of the statistical properties of the turbulence and of the conformity with a random stationary Gaussian process. The two parameters, the scale of turbulence L and the intensity of turbulence σ, used in the analytical representation of turbulence spectra are discussed from the viewpoint of determining numerical values of the parameters by experimental and analytical methods.

SYMBOLS

a_y lateral acceleration, positive to right, g units or ft/sec^2

a_x longitudinal acceleration, positive forward, g units or ft/sec^2

a_n normal acceleration, positive downward, g units or ft/sec^2

g acceleration due to gravity, 32.17 ft/sec^2

$H(\omega)$ frequency-response function

l distance from accelerometer to angle-of-attack and angle-of-sideslip vanes, ft

L scale of turbulence, ft

$R_x(\tau)$ autocovariance function ⎫ autocorrelation function,

$R_x(0)$ autocovariance function at $\tau = 0$ ⎬ $R_x(\tau)/R_x(0)$

r distance, ft

t time, sec

T specified time, sec

V true airspeed, ft/sec

w_a airplane vertical velocity, positive downward, ft/sec

w_g vertical component of gust velocity, positive upward, ft/sec

v_g lateral component of gust velocity, positive to right, ft/sec

u_g longitudinal component of gust velocity, positive in direction of flight path, ft/sec

x arbitrary input disturbance

α_v vane-indicated angle of attack, positive trailing edge up, radians

α_g angle of attack due to gust, positive direction as sketched in figure 2, radians

β_v vane-indicated angle of sideslip, positive trailing edge left, radians

θ pitch angle, positive nose up, radians

$\dot{\theta}$ pitch velocity, positive nose up, radians/sec

λ wavelength, ft

ρ air density, slugs/cu ft

ρ_o sea-level air density, slugs/cu ft

σ root-mean-square deviation

σ_1 root-mean-square deviation determined from area under spectrum

σ_w root-mean-square deviation of vertical component of gust velocity, $\left[R_{w_g}(0)\right]^{1/2}$

τ time lag, sec

Φ_x power spectral density function

ϕ roll attitude, positive right wing down, radians

ψ yaw attitude, positive nose right, radians

$\dot{\psi}$ yaw velocity, positive nose right, radians/sec

ω circular frequency, radians/sec

Ω spatial frequency, ω/V, radians/ft

A bar over a symbol denotes a mean value.

METHOD AND TESTS

General

The power spectra presented herein were determined from measurements made during airplane flight penetrations of the clouds. The power spectra were obtained from Fourier transforms of the autocovariance functions of the time histories of the vertical, lateral, and longitudinal components of true air velocities encountered by the survey airplane. The time histories of true air velocities were in turn obtained from sensors located on a boom extending ahead of the nose of the airplane and corrected for the motions of the sensors themselves. The sensors located on the boom consisted of mass-balanced balsa flow vanes for the vertical and lateral components, and a sensitive airspeed measuring system (pitot-static test head and associated pressure cells) for the longitudinal component. Most of the airplane-sensor motions were measured directly. Details of obtaining the component time histories are given in appendix A.

Airplanes

Jet-propelled airplanes of the fighter and trainer types were used in the cumulus-cloud and severe-storm investigations, respectively. The airplanes were selected on the basis of relatively high structural strength to withstand the intensity of the turbulence expected and on the basis of good handling qualities. With the use of the present method of correcting the flow-vane measurements for airplane motions, the particular airplane used is not significant with respect to the data obtained, since it is used solely as a platform for transporting the instrumentation.

INSTRUMENTATION

Similar instrumentation was installed on each airplane to provide for continuous recording of airflow direction, airspeed, and airplane motions.

The airflow direction was obtained from mass-balanced balsa flow vanes mounted on a boom extending ahead of the nose of the airplane to measure the angle of attack and angle of sideslip. The flow vanes were located approximately 5 feet ahead of the nose for both airplanes. A photograph of the boom installation for the cumulus-cloud airplane is shown in figure 1; the boom installation for the severe-storm airplane was similar.

Airspeed (and altitude) was obtained from an airspeed-altitude recorder in conjunction with a special pitot-static test head installed on the boom forward of the flow vanes. (See fig. 1.) The pressure cells and recorder were located in the nose of the airplane. The resulting tubing, required to run the length of the boom, made necessary a dynamic calibration of the complete airspeed system. (The dynamics of the system had to be properly accounted for in order to determine the longitudinal turbulence spectrum.) The dynamic calibration

was accomplished by impressing sinusoidally varying pressures of known magnitude and frequency on the probe and recording the result.

The natural frequencies of the boom installations were approximately 12 cps for the cumulus-cloud airplane and 14 cps for the severe-storm airplane. The boom natural frequencies were not discernible as such on the flow-vane records of either of the two airplanes. Static boom deflections (both angular and linear) which could produce errors at the airplane short-period stability-mode frequency (approximately 1/2 cps) were measured by applying concentrated loads at the location of the vane transducer masses. Estimates indicated that resulting deflections would produce errors well within the experimental accuracy of the data, and therefore, the effects of boom elasticity were neglected.

Instrumentation for measurement of airplane motions included a three-component recording accelerometer mounted near the center of gravity and recorders for measuring pitching and yawing velocity and angular displacement about the three axes. Secondary instrumentation included a temperature recorder and a statoscope, which is a sensitive device for measuring incremental static pressure. The film speed for all records was approximately one-half inch per second. An 0.1-second interval timer was used to synchronize the various measurements. Two marker switches for indicating events such as cloud entry and precipitation were available to the pilot. The ranges, sensitivities, natural frequencies, and damping of the instruments used for the severe-storm traverses are given in table I, together with the estimated overall accuracy of the recorded quantities. The instrumentation used for the cumulus-cloud traverses was somewhat more sensitive and slightly more accurate for a few of the quantities.

TEST CONDITIONS

Flights were made in both small and large clouds at several altitudes for the two flight investigations. The individual types of investigations are as follows:

Severe-Storm Flights

Table II summarizes the data obtained from the severe-storm flights. The flights were made in the 1960 operations of the National Severe Storms Project. Attempts were made to investigate the variation of turbulence with time in large severe storms, the variation of turbulence with altitude, and the variation of turbulence among the cells of storms or squall lines.

A flight of May 4, 1960, was made as an altitude survey through a single storm area. The altitudes surveyed were 40,000, 35,000, 30,000, and 25,000 feet. Two traverses were made through a severe storm on May 16, 1960. On the first traverse at an altitude of about 38,000 feet, severe hail was encountered. The second traverse was made at 40,000 feet, and again severe hail was encountered. The flight was then aborted because of the hail damage sustained, and the

aircraft returned to base. (One "baseball size" hail dent was found in one of the wing-tip tanks, in addition to damage to air scoops and leading edges.)

Five traverses were made through the storm of May 17, 1960, at an altitude of approximately 39,000 feet. The maximum height of the cloud was about 45,000 feet, and the cloud grew in size from approximately 7 miles in diameter to over 20 miles in diameter during the 38 minutes while the traverses were being made. The time required to complete an individual traverse varied from about 70 to 200 seconds.

Cumulus-Cloud Flights

Table III summarizes the data obtained from the cumulus-cloud flights. Flights were made through small cumulus clouds in the vicinity of Langley Air Force Base, Virginia, to obtain turbulence measurements for small clouds in contrast to the severe storms discussed previously. The flight lengths (in terms of time, as an indication of the cloud diameter) were 26 to 57 seconds as compared with 70 to 300 seconds for the severe-storm flights. An altitude range of 7,000 to 15,000 feet was investigated in nine traverses through four cloud areas.

Loss of Data

Water collected in the test probe and damped out the high-frequency pressure fluctuations; thus, an evaluation of the longitudinal component of gust velocity for all of the severe-storm traverses and all but the first four cumulus-cloud traverses of table III could not be made.

DATA REDUCTION

The data-reduction procedures used involved three steps:

(a) Evaluation of the time histories of the pertinent measurements and combining these time histories to obtain the components of gust velocities

(b) Evaluation of the power spectra of the components

(c) Evaluation of other statistical characteristics of the turbulence time histories, such as root-mean-square gust velocities, probability distribution, and the turbulence scale parameter L

Time Histories

All the measured quantities required for the determination of the vertical, lateral, and longitudinal components of turbulence were read at 0.05-second intervals and combined according to equations (A2), (A3), and (A4) of appendix A. All the quantities under the integral signs were numerically integrated by use

of the trapezoidal rule. This method of integration attenuates the integrated values at the higher frequencies, but this is not considered serious since for the reading interval used the reduction would only be about 5 percent at 2.5 cps. The time histories of the integrated quantities have a predominant frequency in the vicinity of 1/2 cps, with very little "power" beyond a frequency of about 1 cps.

Power Spectra

The general procedure of obtaining power spectra from the time histories is reviewed briefly in appendix A. Details pertinent to this particular investigation are given here. For all the power spectra the time histories were first prewhitened (see ref. 3) by the following procedure:

$$x'(t) = x(t) - x(t - \Delta t)$$

where $x'(t)$ is the prewhitened time history used to determine the autocovariance function and resulting spectrum. The autocovariance functions were determined from 0.05-second interval readings for 60 lags. Although the resulting spectral calculations should yield 61 power estimates uniformly spaced over the frequency range of 0 to 10 cps, the first estimate for zero frequency cannot be determined because of the prewhitening process. There remain, therefore, 60 power estimates for the frequency range of 0.167 cps to 10 cps. This frequency range is considered adequate for airplane response calculations since it usually includes the short-period stability mode and several of the wing structural modes.

In a few cases autocovariance functions were determined from the non-prewhitened time history of the vertical turbulence component by utilizing 0.1-second interval readings and 240 lags. These autocovariance functions were not used to determine spectra (the side lobes of the effective digital "spectral window," or filter, would have introduced too much distortion), but were used in determining the scale parameter L discussed in the following section.

Analytical Representation of Spectra

In application of the spectra to loads or response calculations, it is convenient to represent the spectra by some analytical form. Several analytical representations of turbulence spectra have been used in the past in connection with wind-tunnel turbulence studies (refs. 10 and 11). Two of these representations for transverse velocities are considered in some detail in reference 9 for application to atmospheric turbulence. The expression arrived at for isotropic turbulence whose basic form is attributed to Von Kármán (ref. 12) is:

$$\Phi(\Omega) = \frac{\sigma^2 L}{\pi} \frac{1 + \frac{8}{3}(1.339L\Omega)^2}{\left[1 + (1.339L\Omega)^2\right]^{11/6}} \tag{1}$$

The other spectral representation, which has been used somewhat more extensively for atmospheric turbulence (see refs. 13 and 14, for example), is:

$$\Phi(\Omega) = \frac{\sigma^2 L}{\pi} \frac{1 + 3L^2\Omega^2}{\left(1 + \Omega^2 L^2\right)^2} \tag{2}$$

where for both expressions (1) and (2):

σ^2 mean-square value of turbulence velocity

L   scale of turbulence

Ω spatial frequency defined by $2\pi/\lambda$, where λ is the wavelength of a sinusoidal component

It can be shown that at the higher frequencies (i.e., the frequency range covered by the experimental spectra and of primary importance to conventional aircraft), the spectral power as represented by equation (1) varies in proportion to $\Omega^{-5/3}$, and for equation (2) in proportion to Ω^{-2}. The question then arises as to which of the preceding spectral representations best fits the data, and what means are necessary to determine the parameters σ and L. Various methods of determining these two parameters are discussed in the following paragraphs.

Two different values of the root-mean-square gust velocity σ are useful, as will be seen. The one most easily and accurately obtained from experimental data is simply the square root of the area under the measured spectrum, that is, the truncated values obtained as the square root of the area contained between the low- and high-frequency values of the spectral estimates. The values of σ generally given for the present test data were obtained in this manner and represent good estimates of the relative turbulence intensities represented by the various spectra since they all cover essentially the same range of frequencies.

The other and perhaps more significant value of σ (since it is the one required in analytical representations (1) and (2)) is the square root of the total area under the spectrum extending from zero to infinite frequency. Experimentally this value of σ can only be determined as the square root of the initial value of the autocovariance function $(R_x(0)$ of equation (A6) in appendix A) of the "raw" (that is, non-prewhitened) time history of gust velocity. Several methods of determining a numerical value of L are available and are explored in detail in reference 9. An evaluation of L may be made directly from the truncated power spectrum, assuming either analytical representation (1) or (2), provided $R(0)$, the initial value of the autocovariance function of the non-prewhitened time history, is known.

For analytical representation (1)

$$L = 0.692 \left(\frac{\sigma_w}{\sigma_1}\right)^3 \left(\frac{1}{\Omega_1^{2/3}} - \frac{1}{\Omega_0^{2/3}}\right)^{3/2} \tag{3}$$

8

and for analytical representation (2)

$$L = \frac{3}{\pi}\left(\frac{\sigma_w}{\sigma_1}\right)^2\left(\frac{1}{\Omega_1} - \frac{1}{\Omega_0}\right)$$

(4)

where

$\sigma_w = R(0)^{1/2}$, or the value of σ to zero frequency

σ_1 σ determined from the square root of the area under the truncated spectrum

Ω_1 low-frequency end of the truncated spectrum

Ω_0 high-frequency end of the truncated spectrum

These latter expressions (eqs. (3) and (4)) were used herein to determine values of L from the experimental data since they were convenient to use and resulted in values relatively close to those obtained by the other methods of reference 9.

Additional Turbulence Characteristics

In general, application of power spectra to the calculation of the various responses of airplanes to turbulence is greatly simplified if the turbulence can be considered as a random process characterized by the following properties:

(a) Homogeneity

(b) Stationarity

(c) Gaussian distribution

(d) Isotropy

These properties have been found to apply within limits to clear-air turbulence. (See ref. 14.) Isotropy is briefly discussed in the following paragraph, because the term as applied to atmospheric turbulence is not fully standardized.

Isotropy as applied to atmospheric turbulence is defined herein as the invariance of the statistical characteristics of the turbulence with the airplane flight direction along any horizontal axis. Some indication of isotropy (or the lack of isotropy) can be obtained by the comparison of the various components of the turbulence measured simultaneously during any one traverse. As a consequence of isotropy a definite relation exists between the spectra of fluctuations measured perpendicular to the aircraft flight path (vertical and lateral spectra) and the spectra of the fluctuations measured along the aircraft flight path (longitudinal spectra). This relation presented in reference 14 is

$$\Phi_{w_g}(\Omega) = \Phi_{v_g}(\Omega) = \frac{1}{2}\Phi_{u_g}(\Omega) - \frac{1}{2}\Omega\frac{d\Phi_{u_g}(\Omega)}{d\Omega}$$

(5)

where $\Phi_{w_g}(\Omega)$ and $\Phi_{v_g}(\Omega)$ are the vertical and lateral spectra and $\Phi_{u_g}(\Omega)$ is the longitudinal spectrum. Since equation (5) contains the derivative of the longitudinal spectrum, and experimental spectra generally contain some erratic fluctuations, it is best to fair a smooth curve through the data or fit one of the analytical representations to the data before attempting to use equation (5) to check isotropy. (Eq. (5) is equally applicable to the analytical representation of the turbulence spectrum as given by eq. (1), or to that given by eq. (2).)

RESULTS AND DISCUSSION

The results and discussion are divided into four sections. The first section covers the time histories of the various components of turbulence, and the maximum values obtained in severe storms. The second section is devoted to the spectra obtained; the next section, to some assessment of the homogeneous, stationary, Gaussian, and isotropic characteristics; and the final section, to analytical representation of the spectra, in particular, the scale of turbulence L.

Time Histories

The time histories shown in figure 3 are believed to be the first detailed measurements of the vertical and lateral components of the actual airflow obtained in severe storms. The traverse in figure 3(a) was chosen for illustration because it was quite intense and included portions of the time history outside the visible cloud. In this traverse a predominant up-flow is apparent in the center of the cloud and down-flow near each edge. Some correlation in turbulence intensity appears to exist between the two components. Figure 3(b) illustrates a portion of a traverse of considerably lower intensity at a lower altitude. The portion shown is the roughest part of this particular traverse. The cumulus-cloud traverses present a similar picture, with a considerably lower intensity.

The location of the zero for the two velocity components given in figure 3 is somewhat arbitrary with regard to absolute values of vertical or lateral airflow. The values plotted represent fluctuations about a mean airflow inasmuch as the data-reduction technique was based on incremental values from the mean. (See eq. (A2).) A trend in the time history of the lateral component in figure 3(a), which starts at about -70 ft/sec at cloud entry and ends at approximately 20 ft/sec, may or may not be real, but could result from the data-reduction procedure employed. Such a trend would, of course, affect values of σ obtained from the "raw" time history (square root of initial value of auto-covariance function). In the spectral-data-reduction procedures, however, such effects have been effectively suppressed by the prewhitening procedure used, and do not fall within the frequency range covered by the power spectra. The values of σ_1 thus derived from the areas under these truncated spectra are believed to be essentially free of such effects.

Table II summarizes the results from the severe-storm traverses which have been evaluated from the flights made in 1960. Attention is called to the wide range of maximum gust velocities obtained from the time histories. Of considerable interest is the maximum value of vertical gust velocity of 208 ft/sec encountered in traverse 2 of May 16, 1960. This value represents a peak gust velocity superposed on a large disturbance which had a half wavelength of almost 5,000 feet. At the peak the airplane had a nose-down attitude of about 10° but was rising at a vertical velocity of 83 ft/sec. The vertical acceleration at this point, however, was only about 18 ft/sec/sec. At about this same time severe hail was being encountered, and the lateral turbulence probe (sideslip vane) was damaged by the hail.

Spectra

General characteristics.- The ordinates for all of the spectral plots are given in the unit of $(ft/sec)^2$/radians/ft, with the abscissa being reduced, or spatial, frequency Ω given in radians/ft. The data are plotted against spatial frequency in order to remove the effects of variations in flight speed from run to run. Both the scales are logarithmic. A wavelength scale (reciprocal logarithmic) in feet is also shown for convenience in interpreting the data. As can be seen, the wavelengths covered by the spectra range from about 60 feet to 3,600 feet. The spectra all exhibit similar shapes characterized by decreasing power with increasing frequency. The slightly more erratic appearance of the plots at the high-frequency end results mainly from the closer spacing of the power estimates at this end when shown on a logarithmic scale. (The points are evenly spaced on a linear scale.)

Values of σ_1 for the vertical, lateral, and longitudinal components of gust velocity are shown on the spectral plots and are also given in tables II and III. The values were obtained from the truncated spectra and are directly comparable with each other since they cover essentially the same frequency range. These values of σ_1 are probably of somewhat more value as an indication of relative turbulence intensity for the various traverses (particularly for v_g) than are the maximum and minimum values of gust velocity, since the values of σ_1 are essentially free of uncertainties as to the linear trend effects previously mentioned.

Variations with time, severe storms.- Spectra obtained for five successive traverses of the same storm and at approximately the same altitude are shown in figure 4(a) for the vertical component, and in figure 4(b) for the lateral component. The range of power spectral density $\Phi(\Omega)$ covered by all the curves for this storm is on the order of a factor of 4. The relative intensities of the turbulence for the five traverses are perhaps more apparent from the values of σ_1 for the vertical component of gust velocity plotted in the upper portion of figure 5. These values are plotted against time, from the start of the first traverse. The lower part of the figure shows the extent of the visible cloud at the altitude and time of each traverse. Some correlation of turbulence intensity with rate of cloud growth seems to be indicated, that is, rapid growth at the beginning of the traverse with high intensity for the first traverse and more cloud growth between traverses 3 and 4 with a corresponding increase in σ_1.

Probably the most important indication of figures 4 and 5 is that the power levels vary by a factor of 4 (σ_1 varies by a factor of 2) in essentially the same part of the storm and at the same altitude in a matter of only 20 minutes.

Figure 6 shows spectra of extremely severe turbulence in another storm which persisted at a high level of intensity (σ_1 of 15 to 16 ft/sec) for at least 12 to 15 minutes, and possibly longer. This particular storm of May 16, 1960, is believed to have contained the most severe turbulence ever penetrated by an aircraft from which successful detailed flow measurements were made. Figure 6(a) shows spectra of the vertical and lateral components from traverse 1; and figure 6(b), from traverse 2, which started 12 minutes after traverse 1. Severe hail was encountered on traverse 1, and consequently traverse 2 was made 2,000 feet higher. Severe hail was also encountered on traverse 2, and the aircraft returned to base to be inspected for damage. This storm was growing in height during the time of the traverses. Pilot reports from other aircraft in the area flying level with the top of the storm indicate a height of 42,000 feet at about the start of traverse 1 and approximately 50,000 feet at about the time traverse 2 ended.

Variations with altitude, severe storms.- A flight, made May 4, 1960, surveyed a storm at 5,000-foot-altitude intervals. Figure 7 shows the spectra of the vertical and lateral components obtained at altitudes from 40,000 to 25,000 feet.

Table II gives the local time at the start of each traverse, and as can be seen, approximately 35 minutes elapsed between the start of traverse 1 and the start of traverse 4. After noting the wide variations in intensity possible in 20 minutes or less from data presented in the preceding section, it would seem that little could be concluded from these data as regards intensity variation with altitude of traverse only. The important thing to note, however, is that the turbulence spectra retain approximately the same shape at all altitudes.

Cumulus clouds.- The power-spectral-density curves for the vertical, lateral, and longitudinal components of turbulence in cumulus clouds are shown in figure 8. As can be seen from table III, these spectra were obtained on 4 different days over a period of 6 months during the spring and summer seasons. Blanks in the table are an indication of instrumentation failures or water collecting in the pitot-static head of the sensitive airspeed system as mentioned previously. The cumulus clouds cover a wide range of size and extent of vertical development, and the penetration altitudes ranged from 7,200 feet to 15,000 feet. These spectra exhibit an orderly and rapid decrease in power with increasing frequency similar to the spectra for the severe storms. The level of intensity, however, is generally less than that for the severe-storm turbulence. The range of power at a given frequency is approximately the same for the vertical and lateral components of gust velocity, with the longitudinal component somewhat lower.

It should be noted that the time histories from which the cumulus-cloud spectra were obtained were generally much shorter in length than were those for the severe storms. For this reason, the cumulus-cloud spectra contain somewhat more erratic power fluctuations.

Traverses 4a to 4c (fig. 9) were of special interest in that they were made in a developing cumulonimbus cloud through areas of precipitation and nonprecipitation. Inspection of the records clearly indicated an increase in turbulence level upon entering the precipitation area of the cloud. For this reason, the data were separated into precipitation and nonprecipitation portions. Traverse 4a and traverse 4b were actually parts of the same continuous pass through the cloud, on the same heading and altitude, as noted in table III and figure 9(a). As can be seen in figure 9(a), both the vertical and lateral components of gust velocity for the precipitation portion of the cloud are at a considerably higher power level than are the components for the nonprecipitation portion. Figure 9(b) presents data obtained about 6 minutes later on an approximately reciprocal heading back through the same cloud but at an altitude of about 800 feet lower. Results obtained for the second pass through the cloud are consistent with those obtained for the first pass in that the power for the precipitation area is still appreciably higher for both components. There does not appear to be any consistent difference between the shape of the spectra obtained for precipitation areas as compared with nonprecipitation areas.

Comparisons with clear-air turbulence.- Typical spectra of the various severe-storm and cumulus-cloud spectra just presented are compared with a typical clear-air turbulence spectrum in figure 10. The clear-air turbulence spectrum was obtained from reference 2. These spectra show two general features: the similarity of the slopes of the spectra, and the variation in the intensity of turbulence with weather conditions as indicated by the relative height of the curves. Many samples in each weather condition would undoubtedly yield overlapping bands of spectra. Thus, it appears that turbulence intensity extends over a continuous range of σ from values near zero to relatively large values. (A value of 16 ft/sec for the truncated σ is the maximum measured to date.)

Statistical Characteristics

Homogeneity and stationarity.- As seen in the previous sections, the turbulence varied considerably at different times and locations throughout the storms. In order to investigate the degree of homogeneity and stationarity of the turbulence for measurements as near the same time and location as possible, one of the severe-storm traverses of table II was arbitrarily divided into two equal parts and the spectra of the parts compared. Figure 11 gives this comparison for the vertical component (spectrum of complete traverse previously presented in figure 4(a)). The individual spectra cover a flight distance of approximately 12 miles or 97 seconds each. The two spectra agree in general form but display slight differences in intensity throughout the entire frequency range. It appears, however, that some degree of both homogeneity and stationarity can exist in severe storms. In fact, parts (a) and (b) agree with each other as well as the two parts of a clear-air turbulence traverse examined in the same manner in reference 14.

Gaussian tests.- For the turbulence to be Gaussian the fluctuations of the turbulence must have a normal probability distribution. It has been customary in the past to consider that if a component of the turbulence (vertical

component, for instance) has a normal distribution, then for practical purposes normality of all components of the turbulence is indicated (ignoring higher order Gaussian tests).

The test for a normal distribution for one of the severe-storm traverses is shown in figure 12. All the vertical-component time histories for the flight of May 17, 1960, have been examined in a similar manner, and the particular one shown appears to be representative. The cumulative frequency distribution of the vertical gust velocity, converted to probability, is plotted in the figure. The paper is scaled such that a normal probability distribution plots as a straight line. The data plotted are based on the 0.05-second readings of the vertical-gust-component time history, and a fitted normal distribution is shown as a solid line. The solid line is determined only by the use of σ_w and a standard normal-curve-area table. Note that here the σ used is that determined from the autocovariance function of the raw time history at $\tau = 0$. Values of both σ_w and σ_l are shown in figure 12. It is apparent that the measured data approximate the fitted line quite well except at the extremes of the probability distribution. Such departures of experimental data in these regions are rather common, and for practical purposes the Gaussian approximation appears to be reasonable. (Even the measured distributions for clear-air turbulence depart slightly from a straight line at large values of w_g. See ref. 14, for example.)

Isotropy.- Isotropy requires that the power spectra of the vertical and lateral components (measured simultaneously along the flight path) be equal at all frequencies. (See eq. (5) and previous discussion.) On this basis both the severe-storm and cumulus-cloud data present strong indications of isotropy over the range of wavelengths of about 60 to 3,500 feet.

Figure 13(a) compares spectra of the vertical and lateral components for one of the rougher traverses and for one of the smoother traverses made at 39,000 feet in the storm of May 17, 1960. Figure 13(b) compares the spectra of vertical and lateral components measured in the storm of May 4, 1960, at 25,000 feet. Figures 6(a) and 6(b) compare the spectra for the roughest turbulence encountered in any of the storms. For the case of cumulus clouds, figures 9(a) and 9(b) give similar comparisons for the precipitation and nonprecipitation traverses.

As previously mentioned, longitudinal turbulence measurements were successful for only four of the cumulus-cloud traverses. Of these, only on traverses 1 and 2 were all three components successfully measured. The spectra are presented in figure 13(c) for all three components for traverses 1 and 2. (As far as is known, fig. 13(c) represents the only spectral data available in which all three components were measured simultaneously from an aircraft.) It is apparent that the vertical and lateral spectra are roughly the same with the longitudinal spectrum being somewhat lower than the other two in each case. This relationship is indicated also by the relative values of σ_l. Such a relationship of the spectra over these frequency ranges tends to indicate isotropy according to equation (5).

Equation (5) relates the power of the vertical or lateral component to that of the longitudinal component as follows:

$$\Phi_{w_g}(\Omega) = \Phi_{v_g}(\Omega) = \frac{4}{3} \Phi_{u_g}(\Omega) \tag{6}$$

The preceding relation makes use of equation (1) to represent the spectra of the vertical and lateral components, Φ_{w_g} and Φ_{v_g}, and is valid only in the power drop-off region of the spectra where the power is proportional to $\Omega^{-5/3}$. Thus, the values of σ_1 shown in figure 13(c) (obtained from the areas under the spectra) should be related by:

$$\sigma_{1,w_g} = \sigma_{1,v_g} = \sqrt{\frac{4}{3}} \, \sigma_{1,u_g}$$

The ratios obtained for both traverses are slightly higher than $\sqrt{4/3}$ but the statistical reliability of the two relatively short samples is such that this difference is not believed to be significant.

Analytical Representation

By making use of the two analytical representations of turbulence spectra previously discussed (eqs. (1) and (2)), equations (3) and (4) have been used to obtain numerical values of L, the scale of turbulence. Values of L have been obtained for the spectra of the vertical component of gust velocity for the five thunderstorm traverses of May 17, 1960 (see table II for pertinent details of the traverses), and are given in table IV. The values of σ_w and σ_1 employed in the equations are also given.

By utilizing the experimental data of traverse 4, the various means of obtaining numerical values for L were explored in detail in reference 9. Figure 14 (from ref. 9) presents analytically determined autocorrelation functions compared with the measured autocorrelation of traverse 4. Two different values of L were used for the spectral representation of equation (2). The value of $L = 3,400$ feet approximates the value obtained from the truncated power spectrum by use of equation (4). The value of $L = 4,800$ feet, on the other hand, approximates the value obtained directly from the autocovariance function when it is truncated at a value of r equal to L (essentially the solution of two simultaneous equations, discussed in ref. 9). It can be seen from figure 14 that the curve for $L = 4,800$ feet (spectral representation of eq. (2)) fits the measured autocorrelation about as well as does the curve for $L = 5,600$ feet (spectral representation of eq. (1)). It is apparent that the curve for $L = 3,400$ feet (eq. (2) representation) does not fit at all well.

Figure 15 presents the spectra corresponding to the autocorrelation functions of figure 14. It appears that the spectral representation of equation (1) for $L = 5,600$ feet gives a very good fit to the experimental spectra, whereas the spectral representation of equation (2) provides a poorer fit for either of the values of L as regards slope, with the curve for $L = 3,400$ feet (the worst fit on an autocorrelation basis) producing the better fit.

15

It is thus concluded that the equation (1) spectral representation gives more consistent results and a better fit to both the experimental autocorrelation function and spectrum, at least for this particular sample. In addition, equation (1) gives a better slope fit for all the samples collected to date.

As can be seen from table IV, values of L obtained from equation (3) (eq. (1) spectral representation) ranged from about 2,700 feet to 5,600 feet. Additional work needs to be done on determining values of L, or effectively determining the shape of the power spectra at very long wavelengths, both for severe storms and for clear air.

CONCLUDING REMARKS

An investigation of atmospheric turbulence in cumulus clouds and severe storms has indicated that over the wavelength range of approximately 60 to 3,600 feet, the power spectra are similar in shape to those previously obtained in clear air. Many samples in various weather conditions (clear air, cumulus clouds, and severe storms) would undoubtedly yield overlapping bands of spectra ranging in intensity from the lowest for light clear-air turbulence to the highest for the most severe thunderstorms. The data for severe storms indicated that the power spectral density may vary more nearly in proportion to spatial frequency Ω to the minus five-thirds power at the higher frequencies rather than Ω^{-2} as has sometimes been used in the past for clear-air turbulence studies. Values of L, a quantity required in the analytical representation of the power spectra, may be as large as 5,000 feet for severe-storm turbulence above 25,000 feet in altitude. Additional investigation is needed to more completely define the factors on which L itself depends. Rough evaluations indicated that the turbulence in severe storms can be homogeneous and stationary, isotropic, and Gaussian to a degree comparable with that found in clear-air turbulence. Such assumptions for severe-storm turbulence would probably be valid for many practical applications.

Langley Research Center,
    National Aeronautics and Space Administration,
        Langley Station, Hampton, Va., June 1, 1964.

APPENDIX A

DETERMINATION OF TIME HISTORIES AND SPECTRA

OF TURBULENCE COMPONENTS

Time Histories

Vertical component.- The method used to determine the vertical gust velocities is essentially that employed by references 1 to 5 and is based on flow-direction vane measurements and corrections for the airplane motion. The vertical gust velocity is determined from the vane-indicated angle of attack and airplane motions by the following equation:

$$w_g = V\alpha_v - V\theta - w_a + l\dot{\theta} \tag{A1}$$

A schematic of the airplane flow-vane installation is given in figure 2, showing the axis system and sign convention for the various terms. (Sign convention is also indicated in the symbol list.)

Generally, the measurements were read from a reference on the film records and incremental values were determined by subtracting the mean for the entire record from each individual reading. The airplane vertical velocity could not be measured directly but was determined by integration of the center-of-gravity normal-acceleration measurements. With these modifications, the actual evaluation procedures for the vertical gust velocity are given by

$$w_g = V\left(\alpha_v - \bar{\alpha}_v\right) - V\left(\theta - \bar{\theta}\right) - \int_0^t \left(a_n - \bar{a}_n\right) dt + l\left(\dot{\theta} - \bar{\dot{\theta}}\right) \tag{A2}$$

As a check on the term $\int \left(a_n - \bar{a}_n\right) dt$ in equation (A2) which is of appreciable magnitude in the determination of the vertical component of turbulence, a second integration of the term, yielding the incremental vertical displacement of the airplane, was compared with the indications of a sensitive altimeter (statoscope). The statoscope was first employed to determine a starting and ending point for the integration as far on either side of the storm as the records would allow where the vertical velocity of the airplane was near zero (that is, zero slope for the statoscope time history). Based on this procedure, the quantity $\left(a_n - \bar{a}_n\right)$ was then integrated, thus placing the initial and final condition for the resulting velocity time history at zero. A preliminary second integration was then made, and a new initial condition was determined from the results which would force the final point of the second integration,

$\iint a_n dt\ dt$, to agree with the final point of the sensitive-pressure time history. The two displacement time histories (inertial and pressure derived) were

17

then compared at intermediate points along the traverse. In all cases they agreed quite well at the higher frequencies and down to and including frequencies having a period of 40 to 60 seconds, which was believed to be the phugoid frequency of the airplane. The time histories did, however, tend to drift apart near the center of the traverses, which is believed to be due to a combination of pressure differential within the storm as compared with outside the storm at the same altitude, and to very small errors in the initial and final values of

$\int a_n dt$. (An error of 5 ft/sec in the initial or final value of $\int a_n dt$ will produce an error of 190 feet in the displacement at the midpoint of a 300-second traverse, even when the final point is forced to the correct value by the constant of integration.)

Lateral component.- The reduction of the sideslip-angle measurements to obtain the lateral component of gust velocity is essentially the same as for the vertical component, with the instruments oriented so as to measure the airplane motions in the XY-plane rather than the vertical or XZ-plane. The lateral component of true gust velocity is given by the equation

$$v_g = -V(\beta_v - \bar{\beta}_v) - V(\psi - \bar{\psi}) + l(\dot{\psi} - \dot{\bar{\psi}}) + \int_0^t \left[a_y - \bar{a}_y + 32.2(\phi - \bar{\phi})\right]dt \quad (A3)$$

Longitudinal component.- The longitudinal component of the turbulence is determined from the airspeed and airplane motions and is given by

$$u_g = V' - \int_0^t (a_x - 32.2\theta)dt \quad (A4)$$

where $V' = V - \bar{V}$. The term V' for the longitudinal component was obtained from the fluctuations (about the mean, $\bar{V}$) of the sensitive airspeed system. The last term of equation (A4) which is a correction for the longitudinal response of the aircraft was found to be insignificant for the test airplanes over the frequency range considered herein (0.167 to 10 cps). The omission of this term facilitated corrections to the spectra for the frequency response of the airspeed system. This correction to the longitudinal spectra will be discussed in the next section.

Power Spectra

The time histories of vertical, lateral, and longitudinal components of gust velocities as evaluated by use of equations (A2), (A3), and (A4) were used to obtain the power spectra of atmospheric turbulence. The procedures used were essentially as outlined in references 3 and 13. Basically, the power spectrum of a disturbance $x(t)$ is defined by

$$\Phi_x(\omega) = \frac{2}{\pi} \int_0^\infty R_x(\tau) \cos \omega\tau \, d\tau \quad (A5)$$

18

where $R_x(\tau)$ is the autocovariance function defined by

$$R_x(\tau) = \lim_{T \to \infty} \frac{1}{T} \int_{-T/2}^{T/2} x(t)\, x(t + \tau)\, dt \tag{A6}$$

The numerical procedures used are outlined in reference 3 for obtaining the first raw estimates of power, the final or smoothed estimates, prewhitening of the gust velocity, and the conversion of the prewhitened spectrum to the desired spectrum $\Phi_x(\omega)$.

The determination of the longitudinal spectrum was somewhat different from the determination of the vertical and lateral spectra in that an additional correction was made to the spectrum for the frequency response of the measuring system. The following equation was used for the final determination of the corrected longitudinal spectrum:

$$\Phi_{u_g}(\omega) = \Phi_{V'}(\omega) |H(\omega)|^2 \tag{A7}$$

where Φ_{u_g} is the corrected spectrum, $\Phi_{V'}$ is the spectrum of the fluctuations, and $H(\omega)$ is the frequency response of the airspeed system measured experimentally by the calibration procedure described in the section entitled "Instrumentation."

REFERENCES

1. Chilton, Robert G.: Some Measurements of Atmospheric Turbulence Obtained From Flow-Direction Vanes Mounted on an Airplane. NACA TN 3313, 1954.

2. Crane, Harold L., and Chilton, Robert G.: Measurements of Atmospheric Turbulence Over a Wide Range of Wavelength for One Meteorological Condition. NACA TN 3702, 1956.

3. Coleman, Thomas L., Press, Harry, and Meadows, May T.: An Evaluation of Effects of Flexibility on Wing Strains in Rough Air for a Large Swept-Wing Airplane by Means of Experimentally Determined Frequency-Response Functions With an Assessment of Random-Process Techniques Employed. NASA TR R-70, 1960. (Supersedes NACA TN 4291.)

4. Clementson, Gerhardt C.: An Investigation of the Power Spectral Density of Atmospheric Turbulence. Ph.D. Thesis, M.I.T., 1950.

5. Notess, Charles B., and Eakin, Grady J.: Flight Test Investigation of Turbulence Spectra at Low Altitude Using a Direct Method for Measuring Gust Velocities. Rep. No. VC-839-F-1 (Contract AF 33(616)174), Cornell Aero. Lab., Inc., July 1, 1954.

6. Staff, NSSP: National Severe Storms Project Objectives and Basic Design. Rep. No. 1, Nat. Severe Storms Project, Weather Bur., U.S. Dept. of Commerce, Mar. 1961.

7. Goddard, Brent B.: The Development of Aircraft Investigations of Squall Lines From 1956-1960. Rep. No. 2, Nat. Severe Storms Project, Weather Bur., U.S. Dept. Commerce, Feb. 1962.

8. Steiner, Roy, and Rhyne, Richard H.: Some Measured Characteristics of Severe Storm Turbulence. Rep. No. 10, Nat. Severe Storms Project, Weather Bur., U.S. Dept. Commerce, July 1962.

9. Houbolt, John C., Steiner, Roy, and Pratt, Kermit G.: Dynamic Response of Airplanes to Atmospheric Turbulence Including Flight Data on Input and Response. NASA TR R-199, 1964.

10. Batchelor, G. K.: The Theory of Homogeneous Turbulence. Cambridge Univ. Press, 1953.

11. Dryden, Hugh L.: Turbulence Investigations at the National Bureau of Standards. Proc. Fifth Int. Cong. Appl. Mech. (Cambridge, Mass., 1938), John Wiley & Sons, Inc., 1939, pp. 362-368.

12. Von Kármán, Theodore: Progress in the Statistical Theory of Turbulence. Collected Works of Theodore von Kármán, vol. IV, 1940-1951. Butterworths Sci. Publ.(London), 1956, pp. 362-371.

13. Press, Harry, and Tukey, John W.: Power Spectral Methods of Analysis and Their Application to Problems in Airplane Dynamics. Vol. IV of AGARD Flight Test Manual, Pt. IVC, Enoch J. Durbin, ed., North Atlantic Treaty Organization (Paris), pp. IVC:1 - IVC:41.

14. Press, Harry: Atmospheric Turbulence Environment With Special Reference to Continuous Turbulence. Rep. 115, AGARD, North Atlantic Treaty Organization (Paris), Apr.-May 1957.

TABLE I

INSTRUMENT CHARACTERISTICS

Quantity measured and units	Range	Recording sensitivity, units per in. of film deflection	Natural frequency, f_n, cps, of –		Approximate damping ratio of –		Estimated accuracy of recorded quantities
			Sensing element	Recording element	Sensing element	Recording element	
Normal acceleration, g units	±2	2.09	19	(a)	0.66	(a)	0.04
Lateral acceleration, g units	±1	1.96	20	(a)	0.66	(a)	0.02
Longitudinal acceleration, g units	±1	2.08	20	(a)	0.66	(a)	0.02
Pitch velocity, radians/sec	±1	0.96	14	(a)	0.65	(a)	0.02
Yaw velocity, radians/sec	±0.5	0.49	14	(a)	0.66	(a)	0.01
Pitch attitude, radians	±0.17	0.19	(b)	(a)	(b)	(a)	0.001
Roll attitude, radians	±0.52	0.94	(c)	100	(c)	0.65	0.0052
Yaw attitude, radians	±0.35	0.59	(c)	110	(c)	0.65	0.0035
Vane-indicated angle of attack, radians	±0.20	0.43	[d]48	115	[e]$0.7\sqrt{\frac{\rho}{\rho_0}}$	0.65	0.002
Vane-indicated angle of sideslip, radians	±0.20	0.46	[d]48	105	[e]$0.7\sqrt{\frac{\rho}{\rho_0}}$	0.65	0.002
Impact pressure, psf	0 to 600	[f]69 to 77	[g]7.6	---	[g]0.47	----	0.60
Static pressure, psf	0 to 2,200	[f]153 to 320					2.2
Incremental static pressure, inches of water	7 to -9	[f]1.6 to 3.1					0.032
Time, sec	0.10-sec pulse	[h]2.0					

[a]Direct optical recording, $f_n \gg 10$ cps.

[b]Attitude gyro with optical "pickoff," $f_n \gg 10$ cps.

[c]Attitude gyro with electrical "pickoff," $f_n \gg 10$ cps.

[d]For 210 knots indicated airspeed.

[e]Approximate only.

[f]The approximate range of slope is given, since the calibration is nonlinear.

[g]For complete pitot-static system and recorder installed in airplane used in cumulus-cloud traverses (sea-level conditions).

[h]Approximate film speed for all recorders, 1/2 inch per second.

TABLE II

SUMMARY OF SEVERE-STORM TRAVERSES

Date	Traverse (a)	Average pressure altitude, ft	True heading, deg (b)	Average true airspeed, ft/sec	Duration of traverse, sec	Time range covered by power spectra, sec	Local time at start of traverse, CST	Estimated cloud height, ft	Precipitation encountered	Maximum w_g, ft/sec Up	Maximum w_g, ft/sec Down	Maximum v_g, ft/sec Right	Maximum v_g, ft/sec Left	σ_1, ft/sec, for w_g	σ_1, ft/sec, for v_g
May 4, 1960	1	40,000	225	635	239	214	1548	40,000+	Yes	56	-62	76	-59	9.73	10.81
	2	35,000	070	625	308	304	1604	40,000+	No	51	-78	47	-70	6.64	6.78
	3	30,000	220	595	220	210	1615	40,000+	No	38	-44	67	-50	6.14	6.76
	4	25,000	060	540	258	255	1623	40,000+	Yes	92	-31	84	-64	6.48	6.05
May 16, 1960	1	38,000	180	660	290	177	1724	42,000	Yes	141	-105	104	-146	15.55	16.17
	2	40,000	340	660	198	139 c84	1736	50,000	Yes	208	-124	87	-93	15.33	14.31
May 17, 1960	1	39,000	170	686	72	56	1622	45,000	Yes	74	-110	66	-94	16.02	15.39
	2	39,000	210	650	147	147	1629	45,000	No	95	-89	107	-82	13.62	12.14
	3	39,000	180	660	152	152	1642	45,000	No	48	-47	57	-56	7.46	9.00
	4	39,000	340	665	195	195	1651	45,000	Yes	130	-99	85	-94	13.38	13.17
	5	39,000	160	645	202	202	1656	45,000	No	49	-50	92	-66	8.57	8.84

[a]Corresponds to numbers shown on figures.

[b]Approximate heading flown by pilot as taken from tape transcripts of in-flight voice communication.

[c]Hail damage caused loss of lateral sensor (sideslip vane) during traverse.

TABLE III

SUMMARY OF CUMULUS-CLOUD TRAVERSES

Date	Traverse (a) Flight	Traverse (a) Sequence	Average pressure altitude, ft	True heading, deg (b)	Average true airspeed, ft/sec	Duration of traverse, sec	Local time at start of traverse, EST	Estimated cloud height, ft	Estimated cloud base, ft	Precipitation encountered	σ_1, ft/sec for w_g	σ_1, ft/sec for v_g	σ_1, ft/sec for u_g
Mar. 6, 1959	1		7,200	030	453	36.0	1238	9,000	4,000	No	7.82	7.77	5.49
May 19, 1959	2		11,300	020	495	55.4	1510	14,000	4,000	No	6.14	5.63	4.52
May 21, 1959	3	a	12,700	330	525	57.0	1500	18,000	8,000	No	4.29	----	3.03
		b	10,000	150	495	44.0	1502	------	-----	No	5.40	----	2.83
Aug. 5, 1959	4	a	15,000	040	525	26.0	1525	20,000	1,500	Yes	8.35	8.53	----
		b	15,000	040	525	42.4	------	------	-----	No	4.17	5.06	----
		c	14,200	210	520	31.0	1531	------	-----	No	3.39	4.03	----
		d	14,200	210	520	47.0	------	------	-----	Yes	8.53	8.16	----
		e	13,200	035	510	51.0	1535	------	-----	Yes	9.16	7.91	----

[a]Corresponds to number shown on figures.

[b]Approximate heading flown by pilot as taken from tape transcripts of in-flight voice communication.

TABLE IV

VALUES OF L OBTAINED FROM SEVERE-STORM TRAVERSES ON MAY 17, 1960,

FOR USE IN ANALYTICAL REPRESENTATION OF TURBULENCE SPECTRA

Traverse	σ_w, ft/sec	σ_l, ft/sec	L, ft, from -	
			Eq. (3)	Eq. (4)
1	34.99	16.02	4,260	2,940
2	27.20	13.62	3,080	2,320
3	14.47	7.46	2,870	2,230
4	32.33	13.38	5,620	3,480
5	16.39	8.57	2,710	2,120
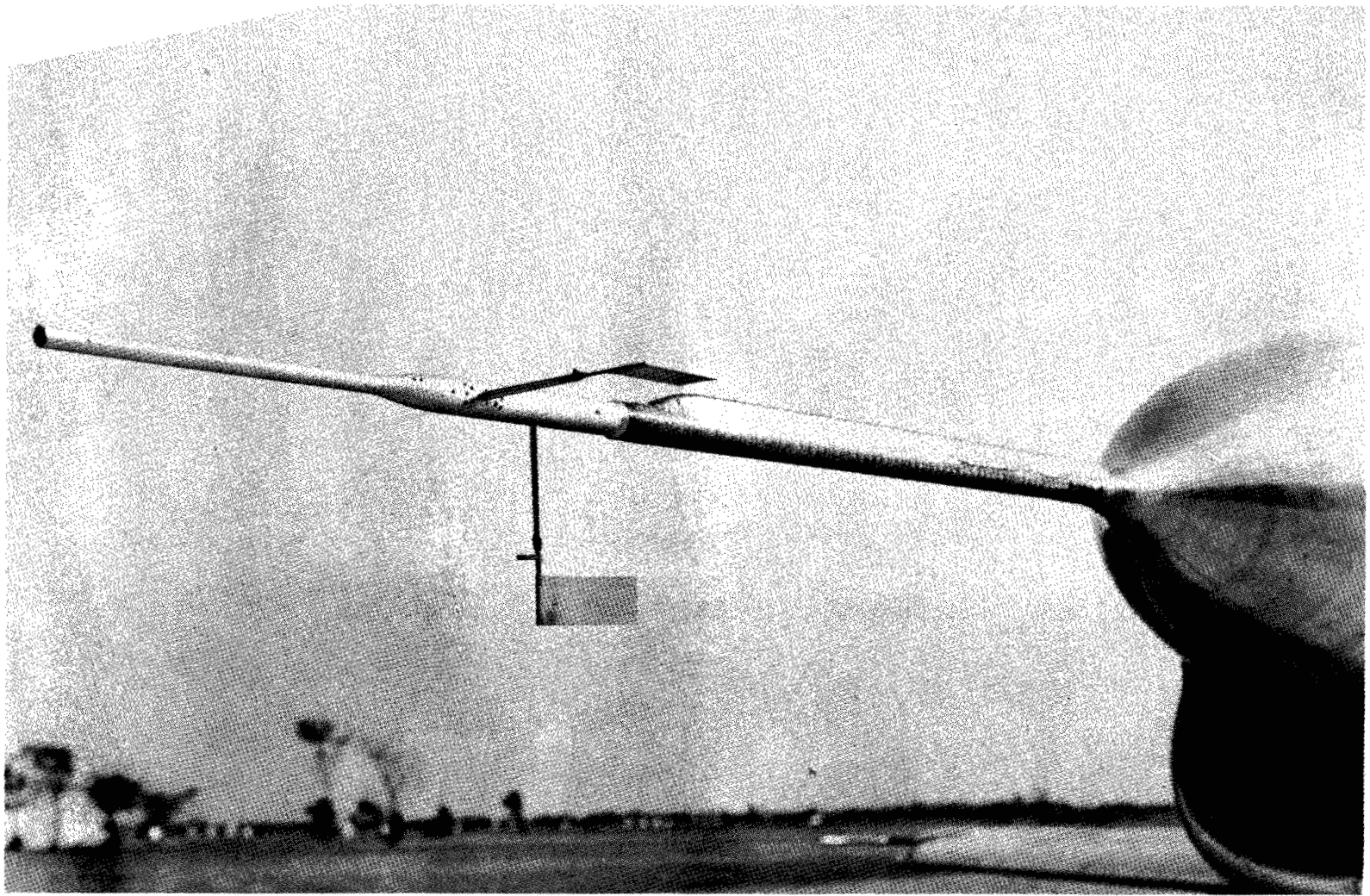
Figure 1.- Flow-vane and pitot-static installation.
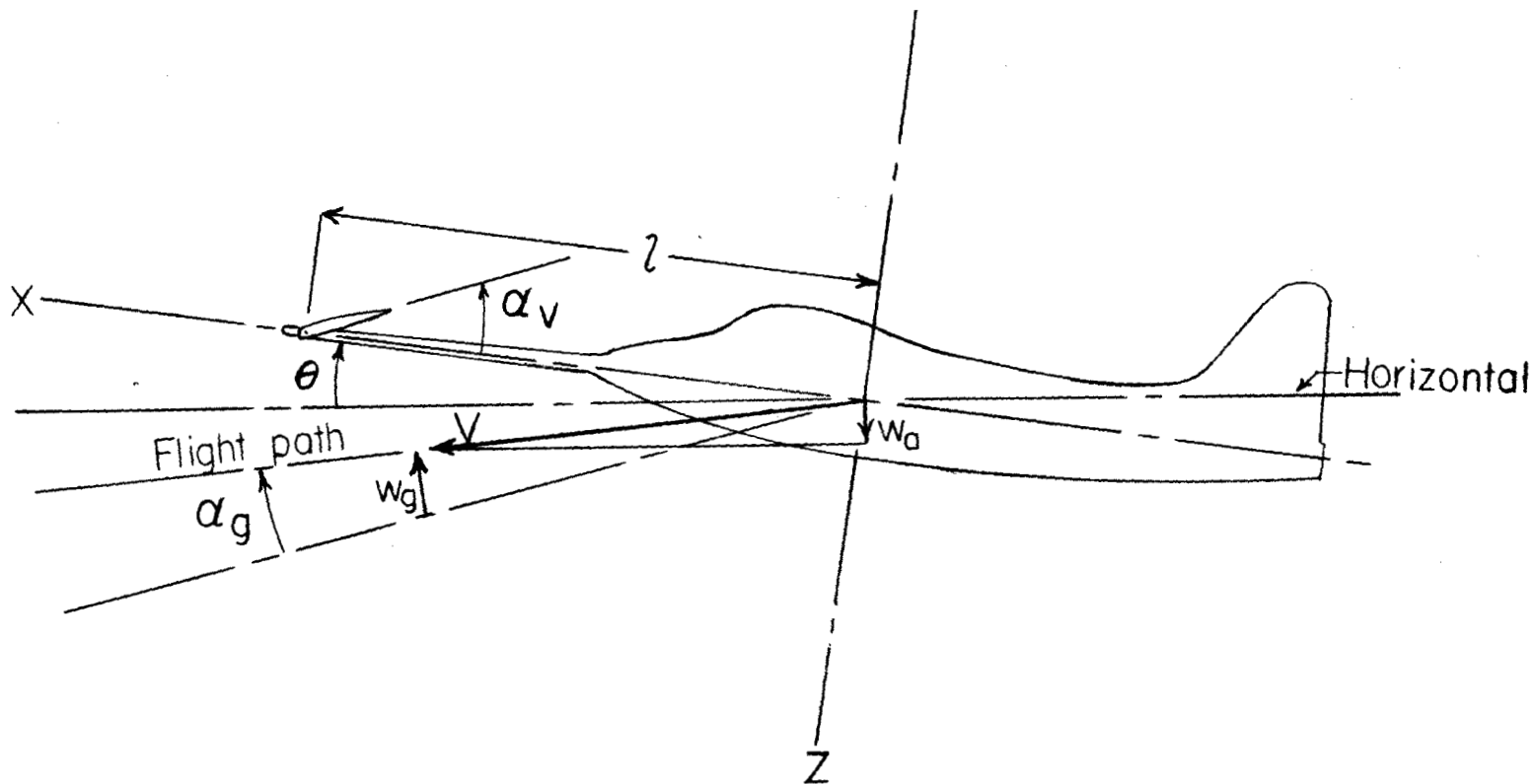
Figure 2.- Schematic of airplane flow-vane installation, showing axis system and sign convention. Positive direction of angles and velocities is shown.
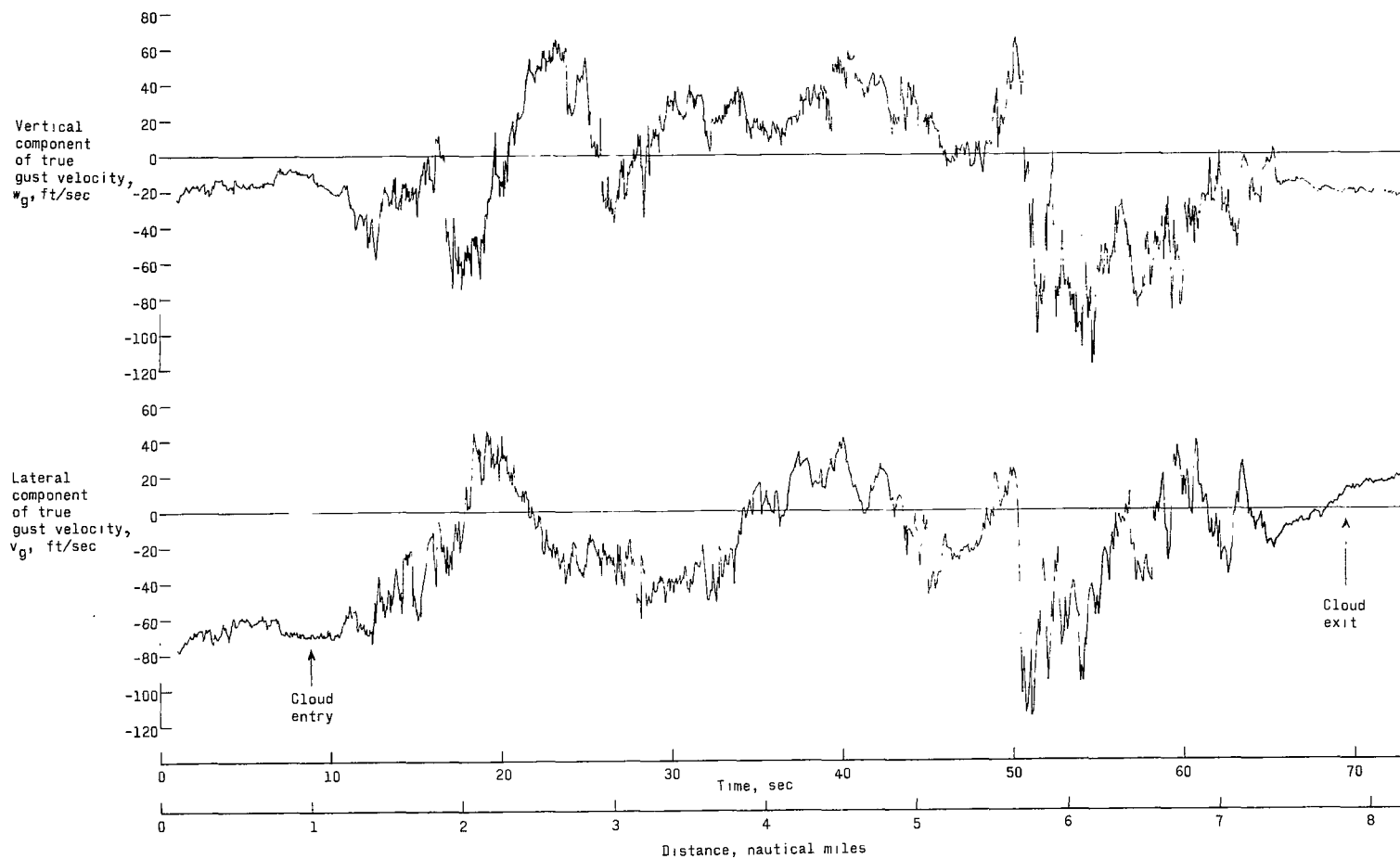
(a) Time histories of vertical and lateral gust components; traverse 1, altitude of 39,000 feet, May 17, 1960.

Figure 3.- Sample turbulence measurements.
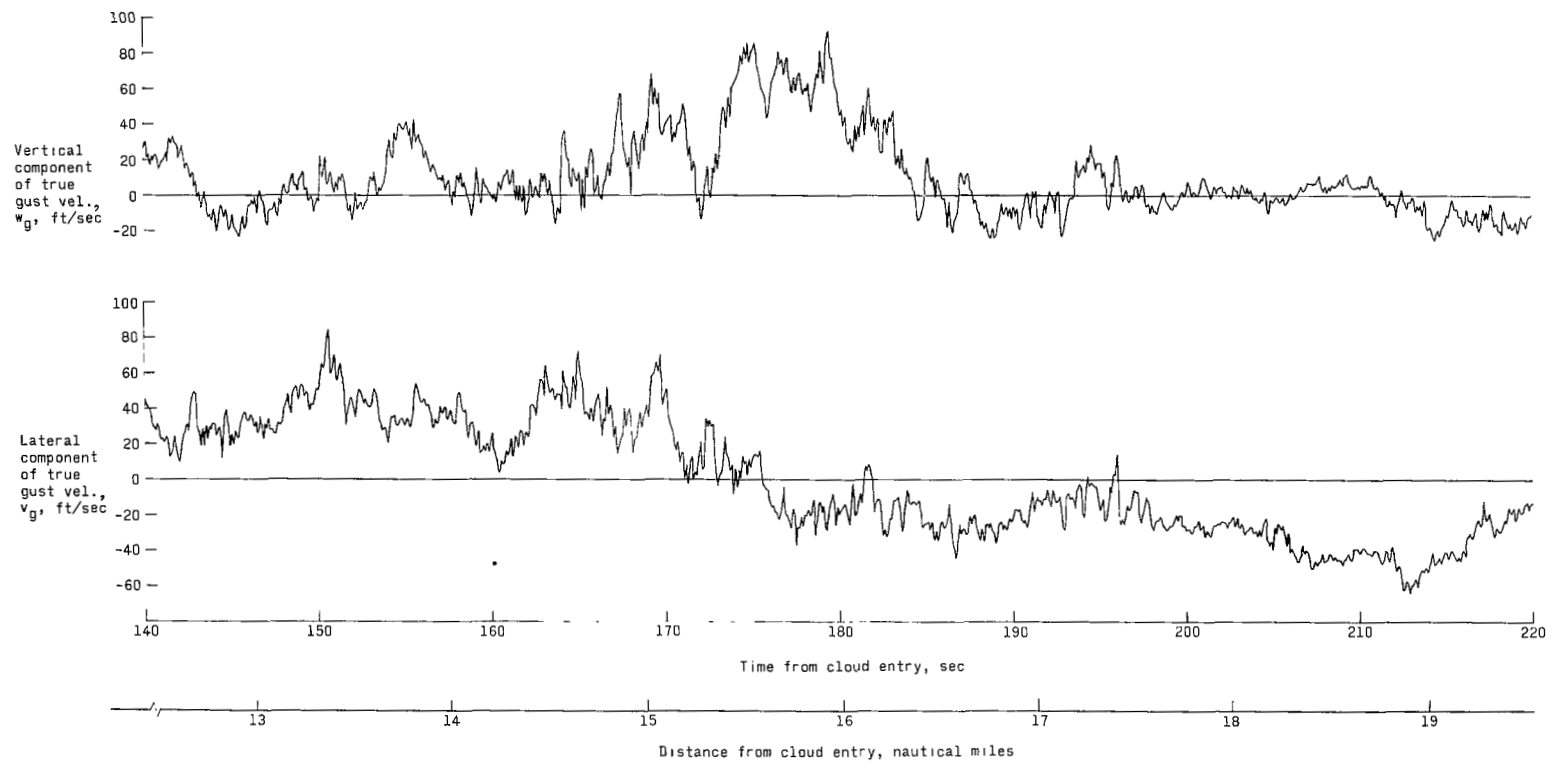
(b) Portion of time histories of vertical and lateral gust components; altitude of 25,000 feet, May 4, 1960.

Figure 3.- Concluded.
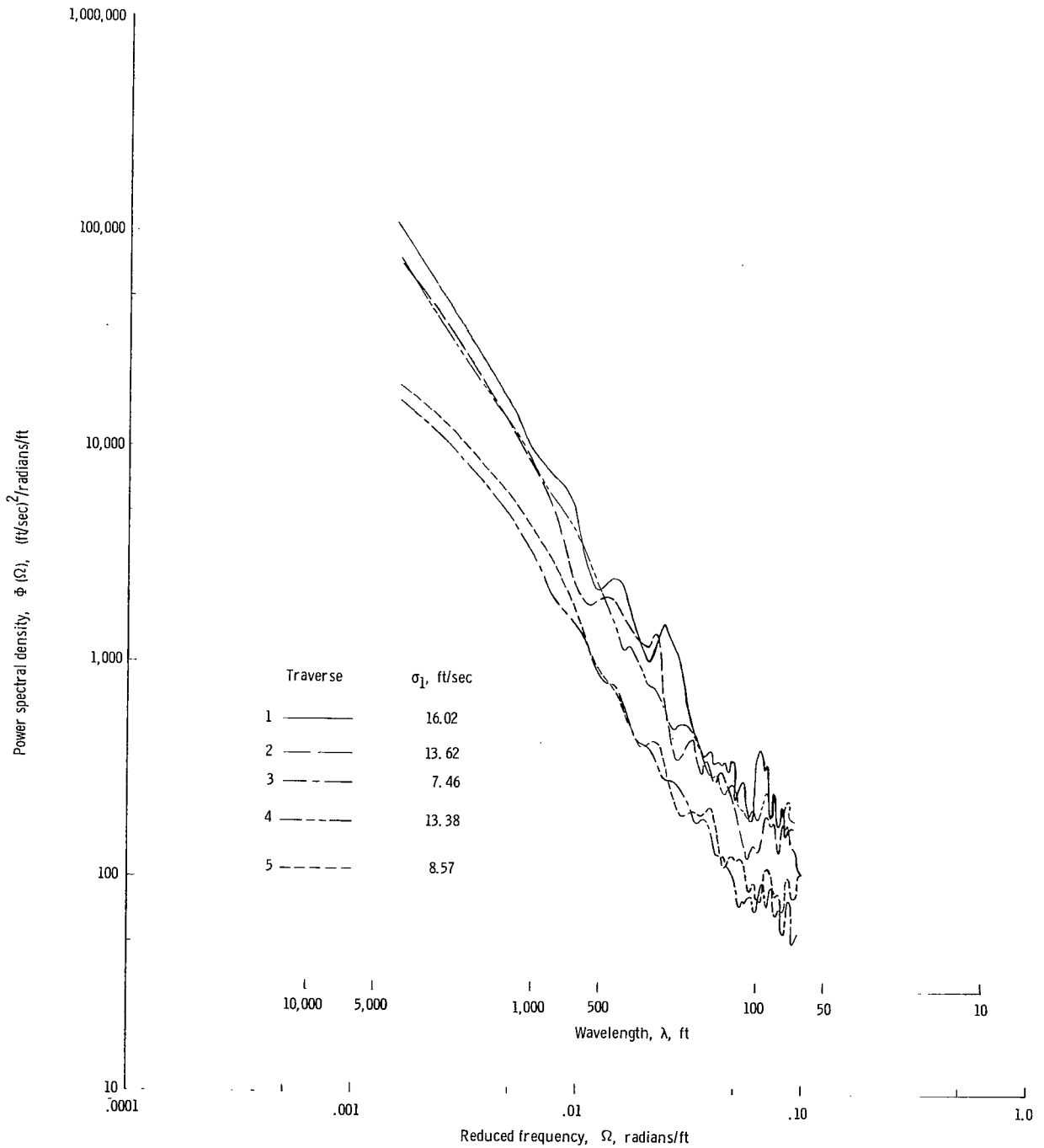
(a) Vertical component.

Figure 4.- Comparison of power spectra of turbulence measured in successive traverses of severe storm of May 17, 1960; altitude of 39,000 feet.
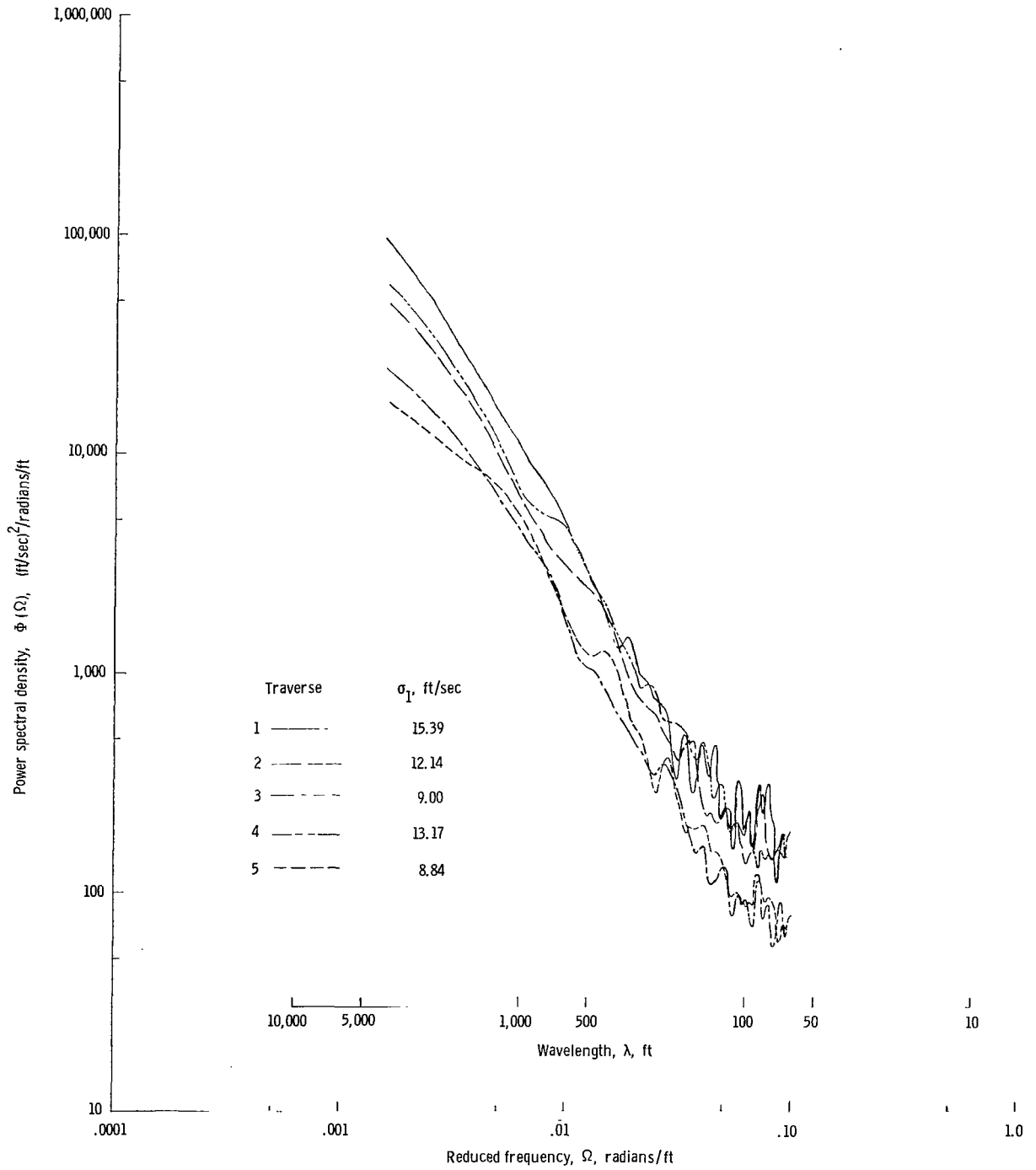
(b) Lateral component.

Figure 4.- Concluded.
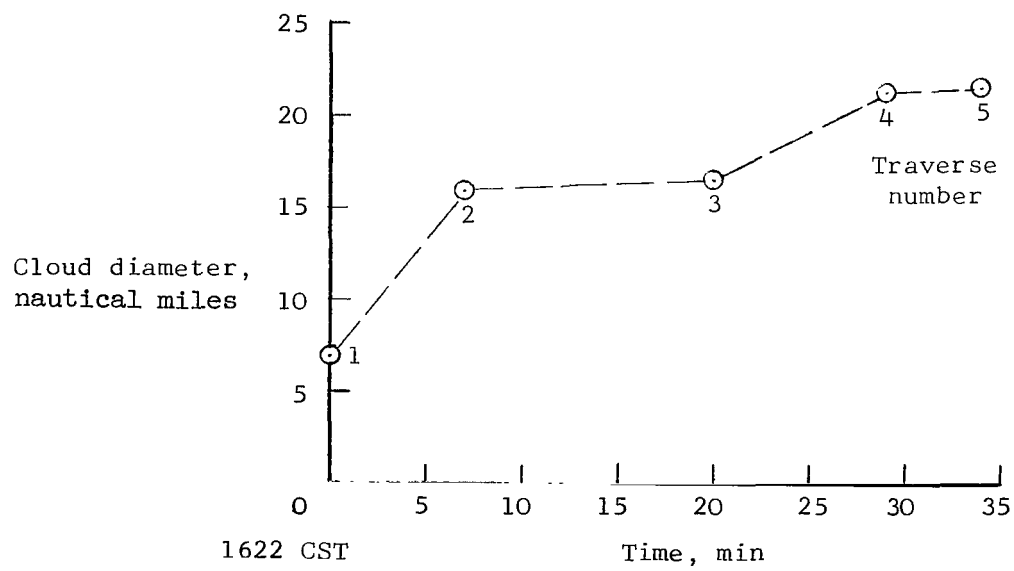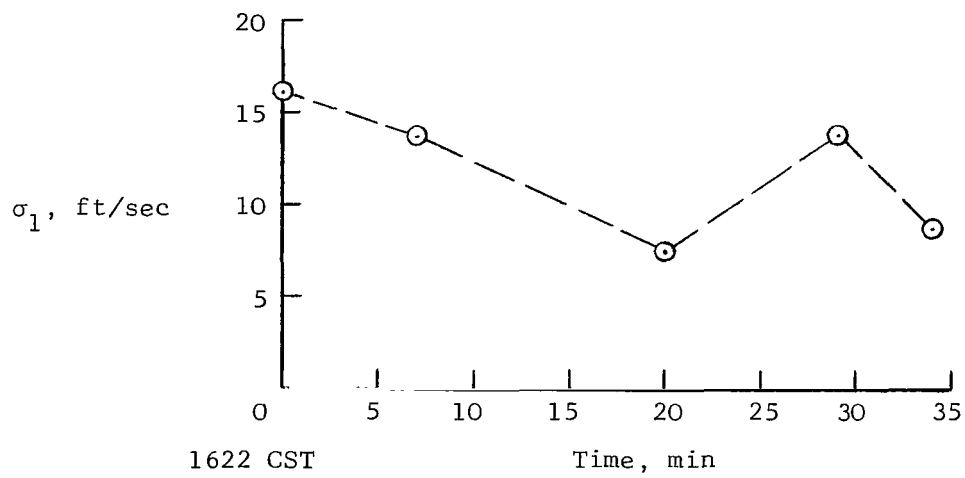
Figure 5.- Variation of vertical component of turbulence intensity and cloud diameter with time at 39,000-foot altitude in severe storm of May 17, 1960.

31
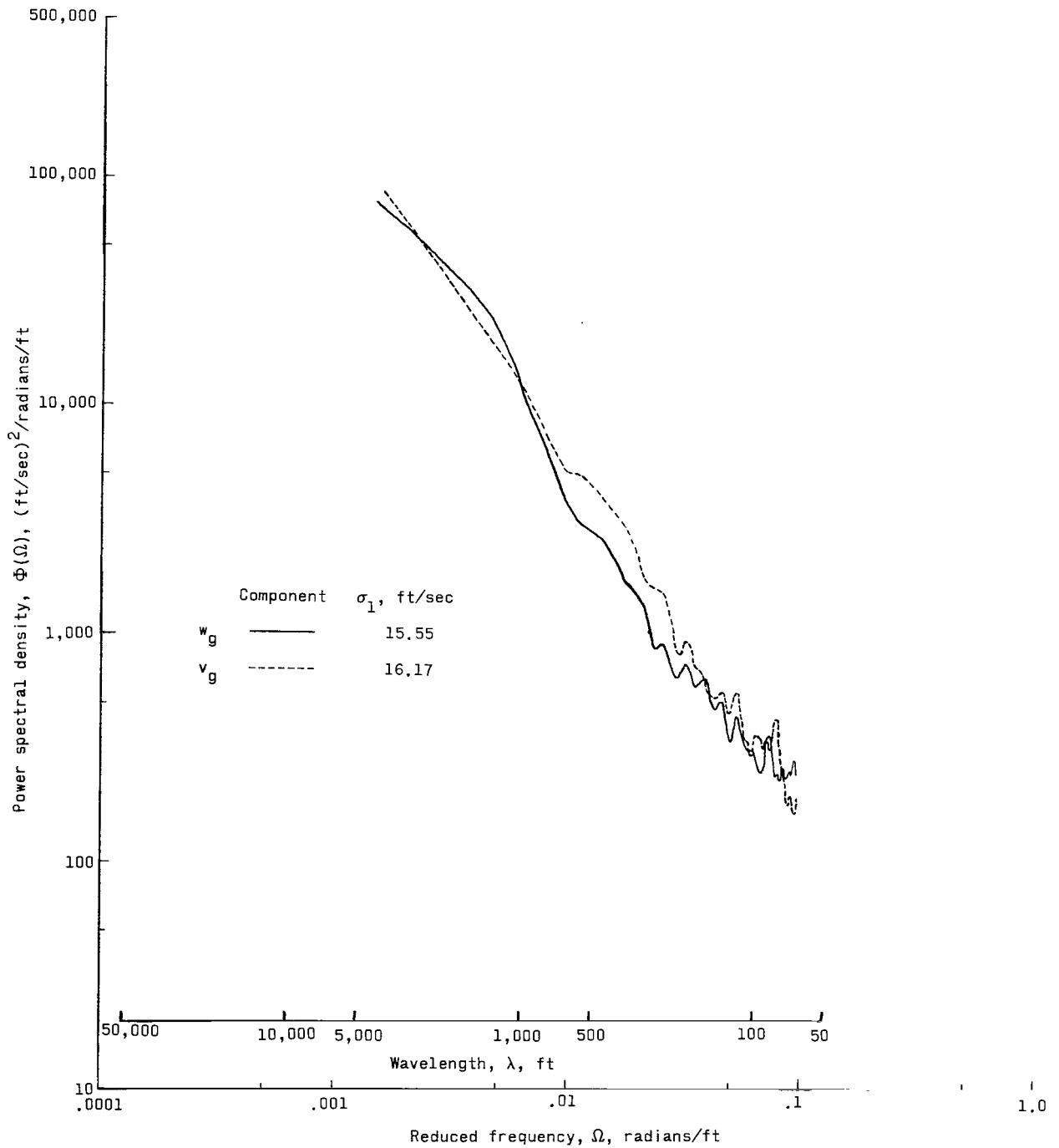
(a) Traverse 1, 38,000-foot altitude.

Figure 6.- Comparison of power spectra of the vertical and lateral components of turbulence measured in severe storm of May 16, 1960.
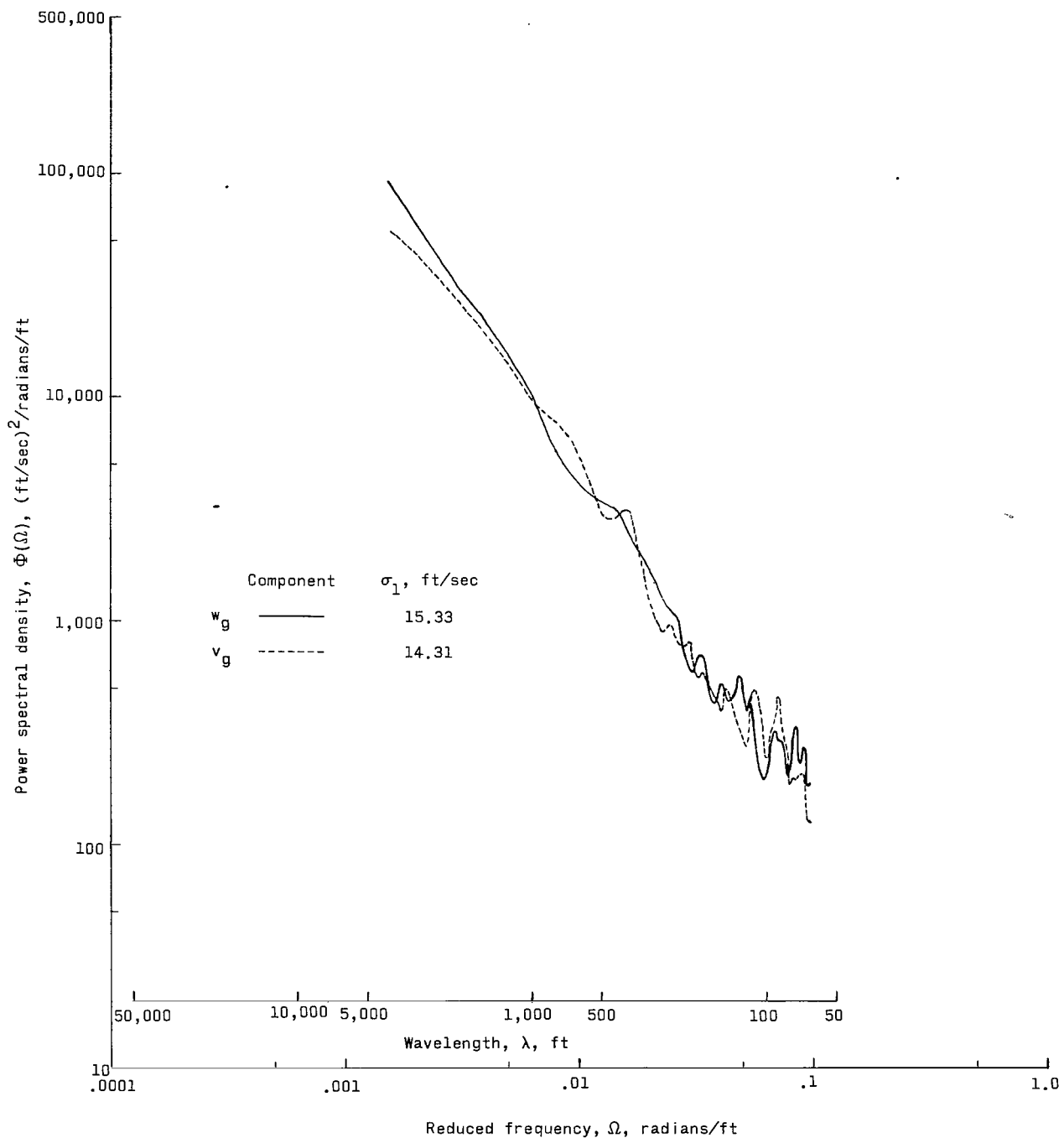
(b) Traverse 2, 40,000-foot altitude.

Figure 6.- Concluded.
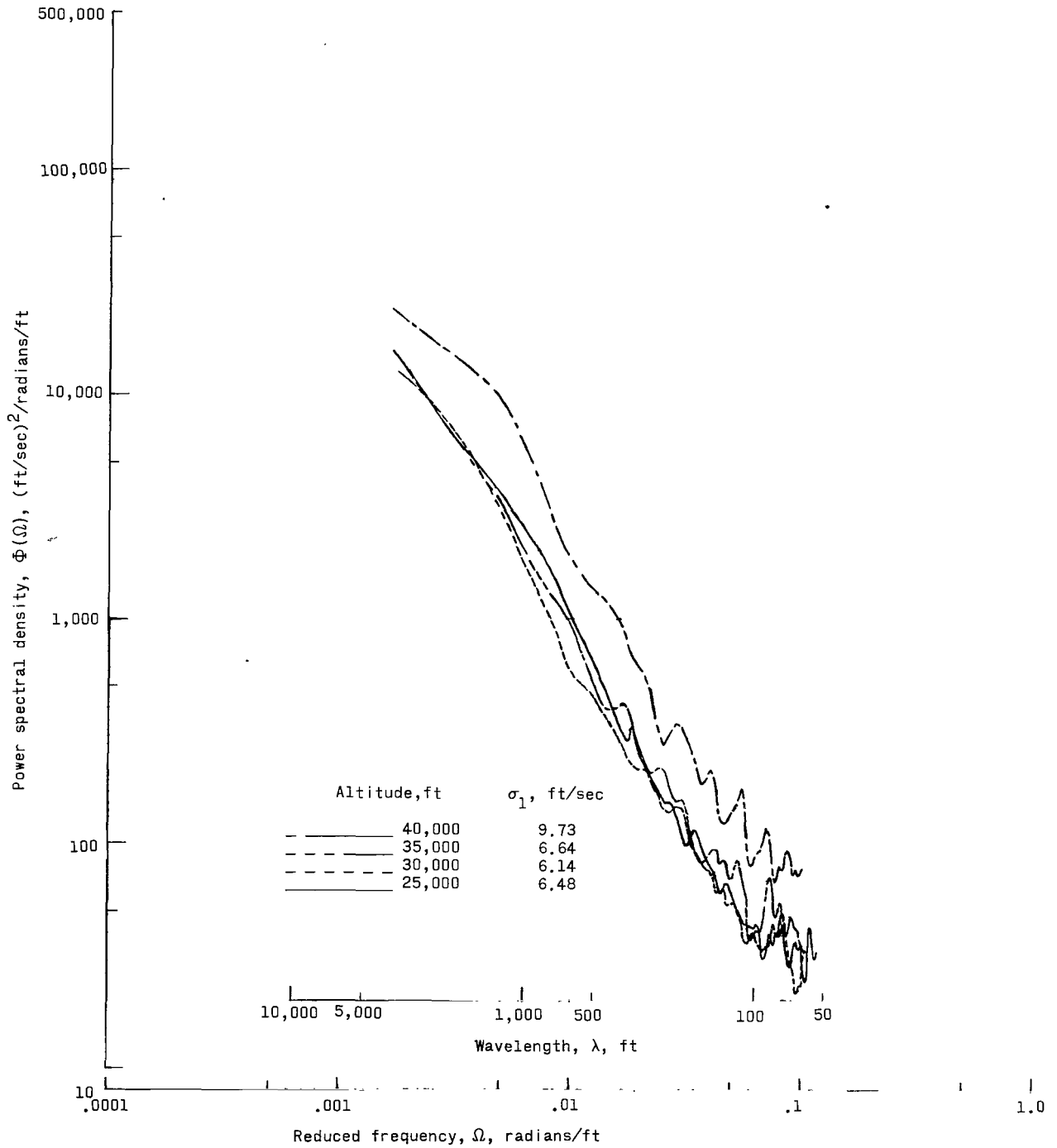
(a) Vertical component.

Figure 7.- Comparison of power spectra of turbulence measured in successive altitude traverses of severe storm of May 4, 1960.
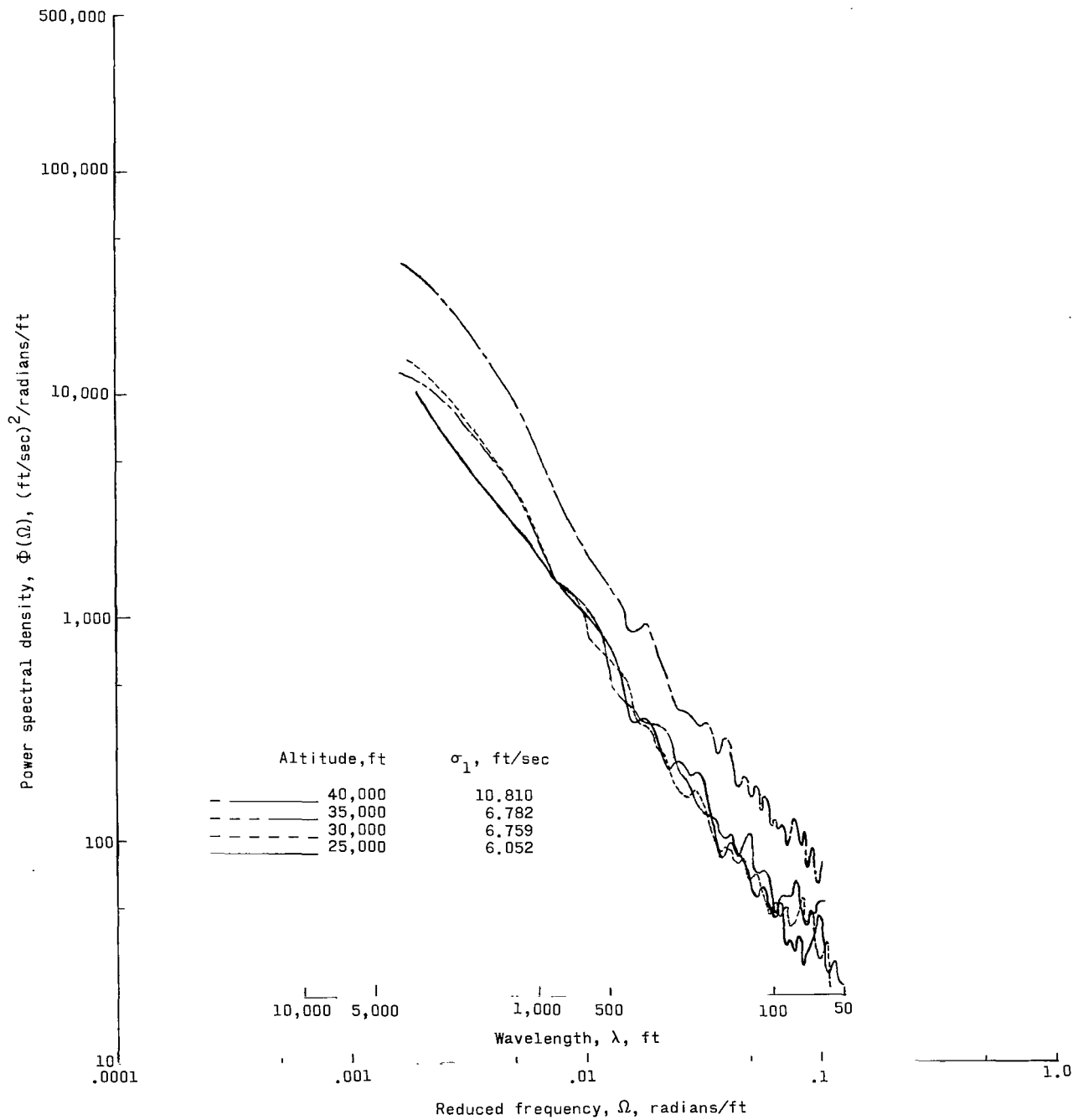
(b) Lateral component.

Figure 7.- Concluded.

Legend:

Traverse	σ_1, ft/sec
1	7.82
2	6.14
3-a	4.29
3-b	5.40
4-a	8.35
4-b	4.17
4-c	3.39
4-d	8.53
4-e	9.16
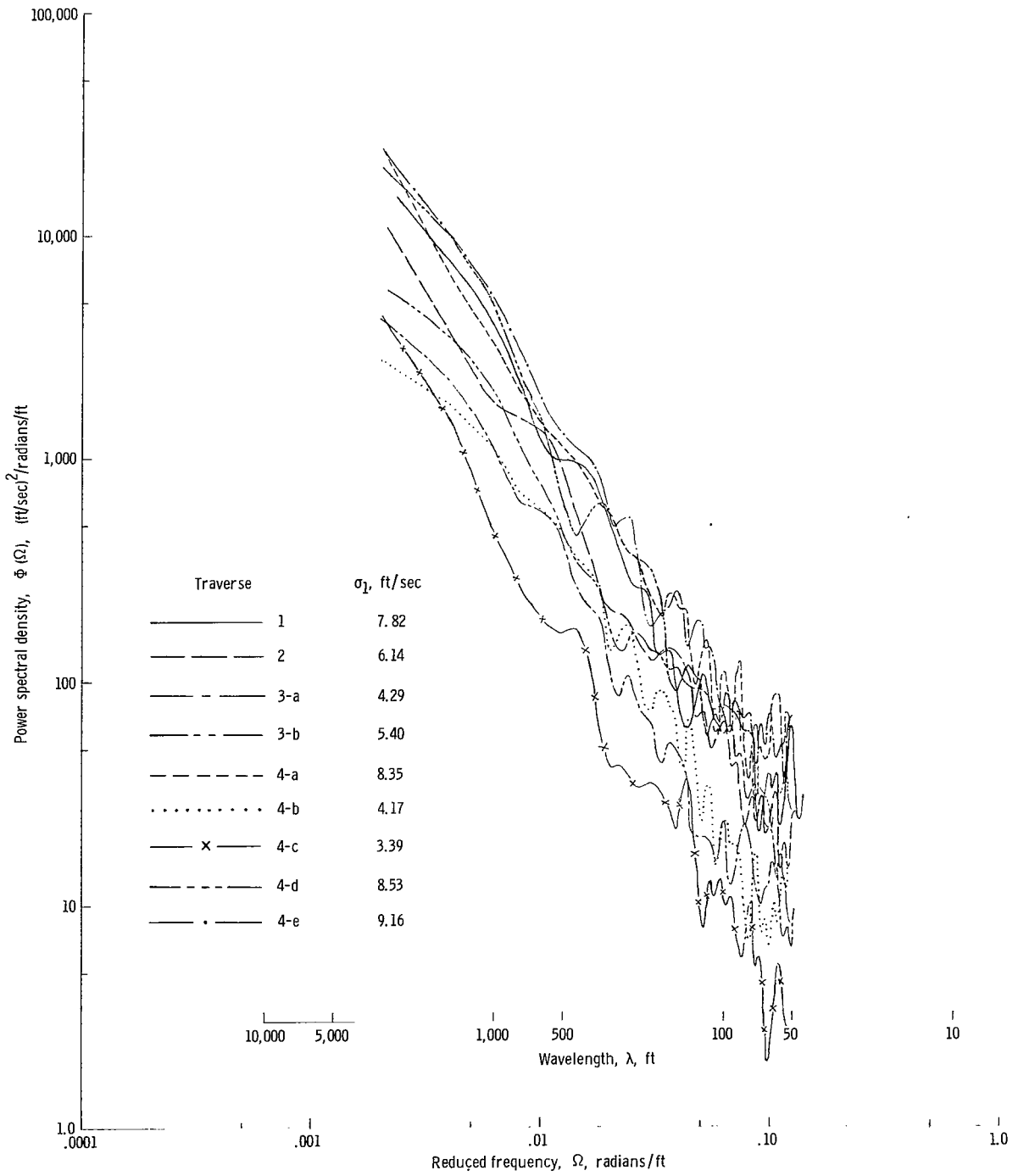
(a) Vertical component.

Figure 8.- Comparison of power spectra of turbulence measured in cumulus clouds.

100,000

10,000

1,000

Power spectral density, $\Phi(\Omega)$, $(ft/sec)^2/radians/ft$

100

10

1.0

Traverse	σ_1, ft/sec
1	7.77
2	5.63
4-a	8.53
4-b	5.06
4-c	4.03
4-d	8.16
4-e	7.91

Wavelength, λ, ft

10,000   5,000   1,000   500   100   50   10

.0001   .001   .01   .10   1.0

Reduced frequency, Ω, radians/ft
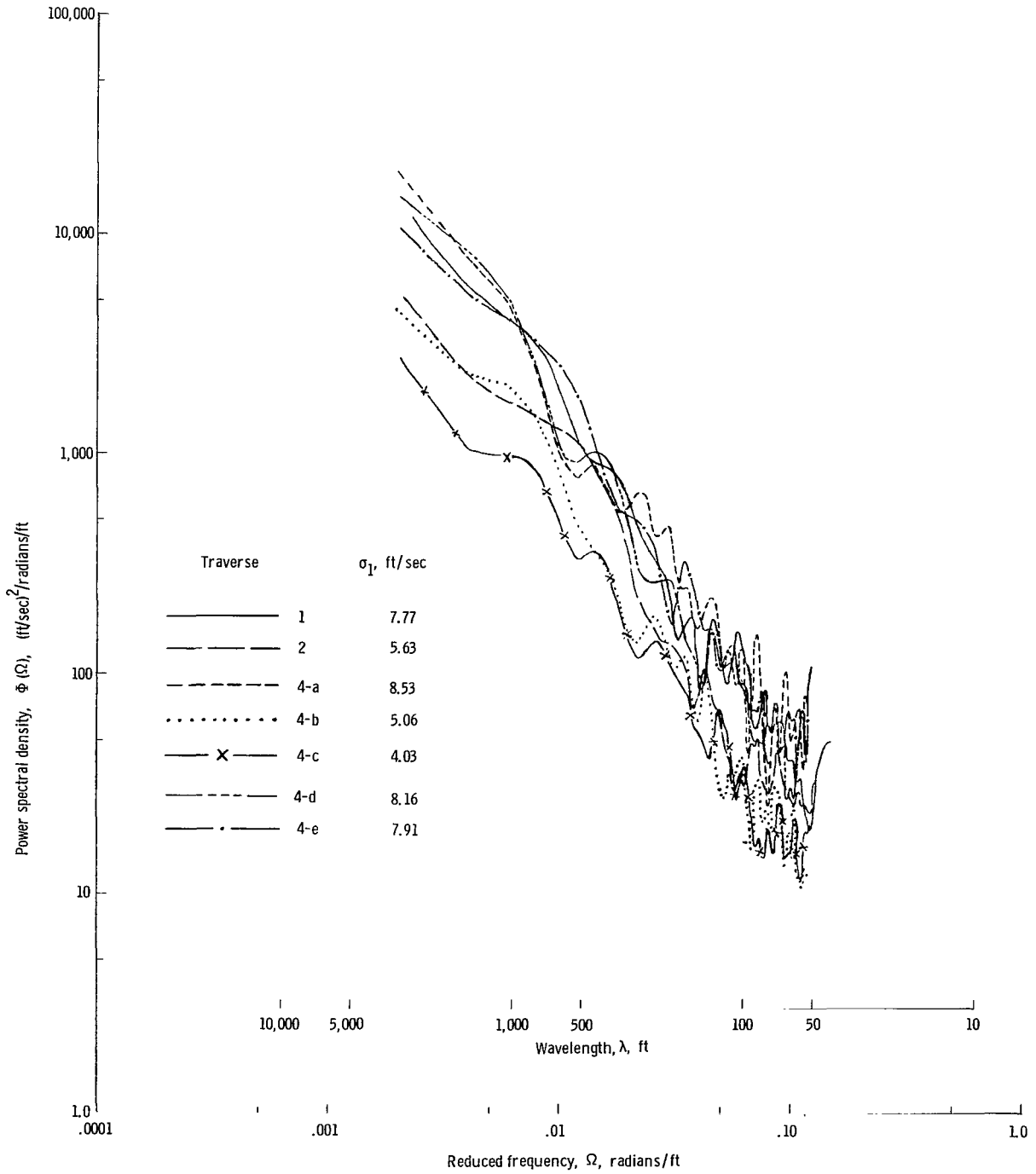
(b) Lateral component.

Figure 8.- Continued.

37
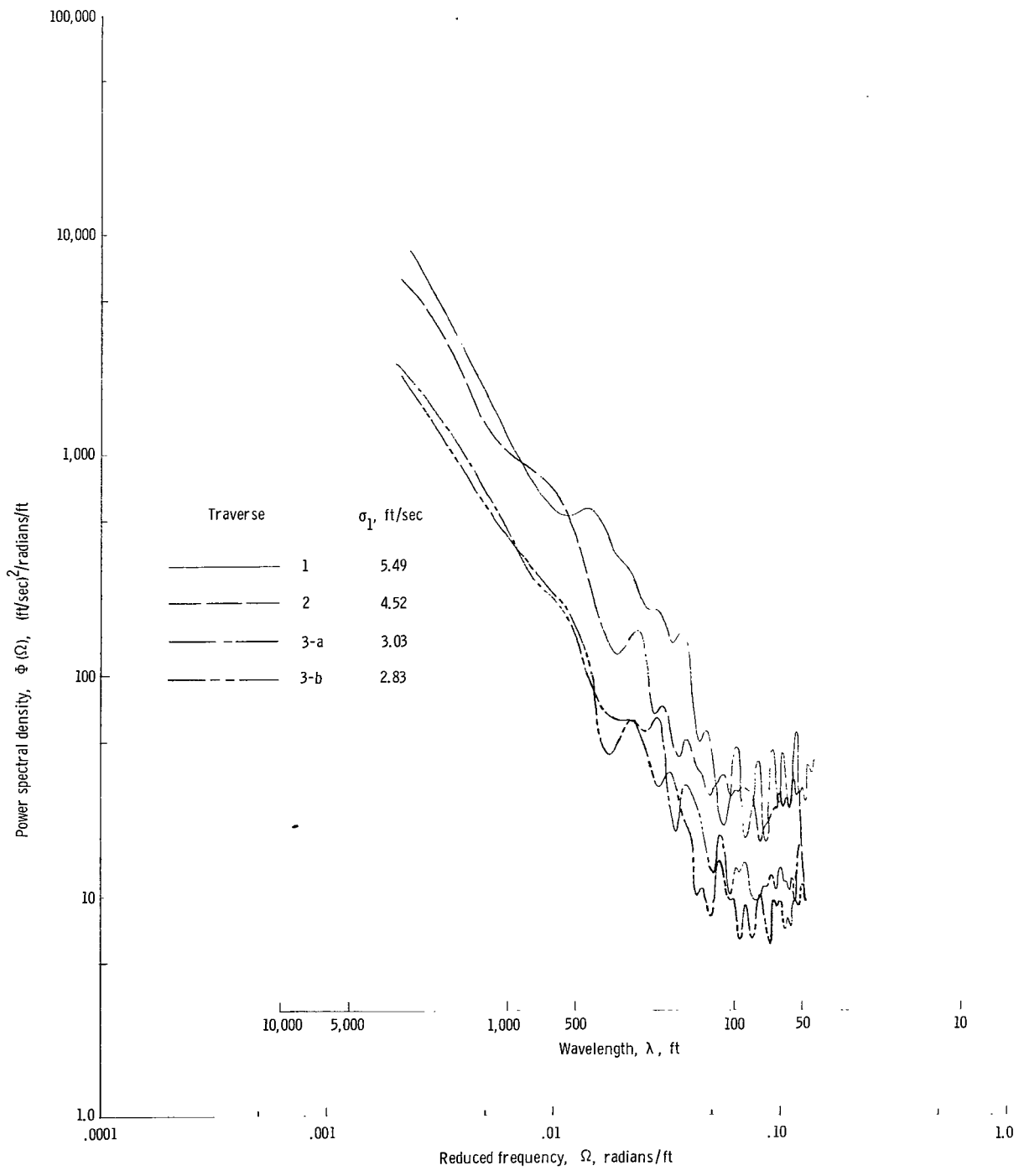
(c) Longitudinal component.

Figure 8.- Concluded.
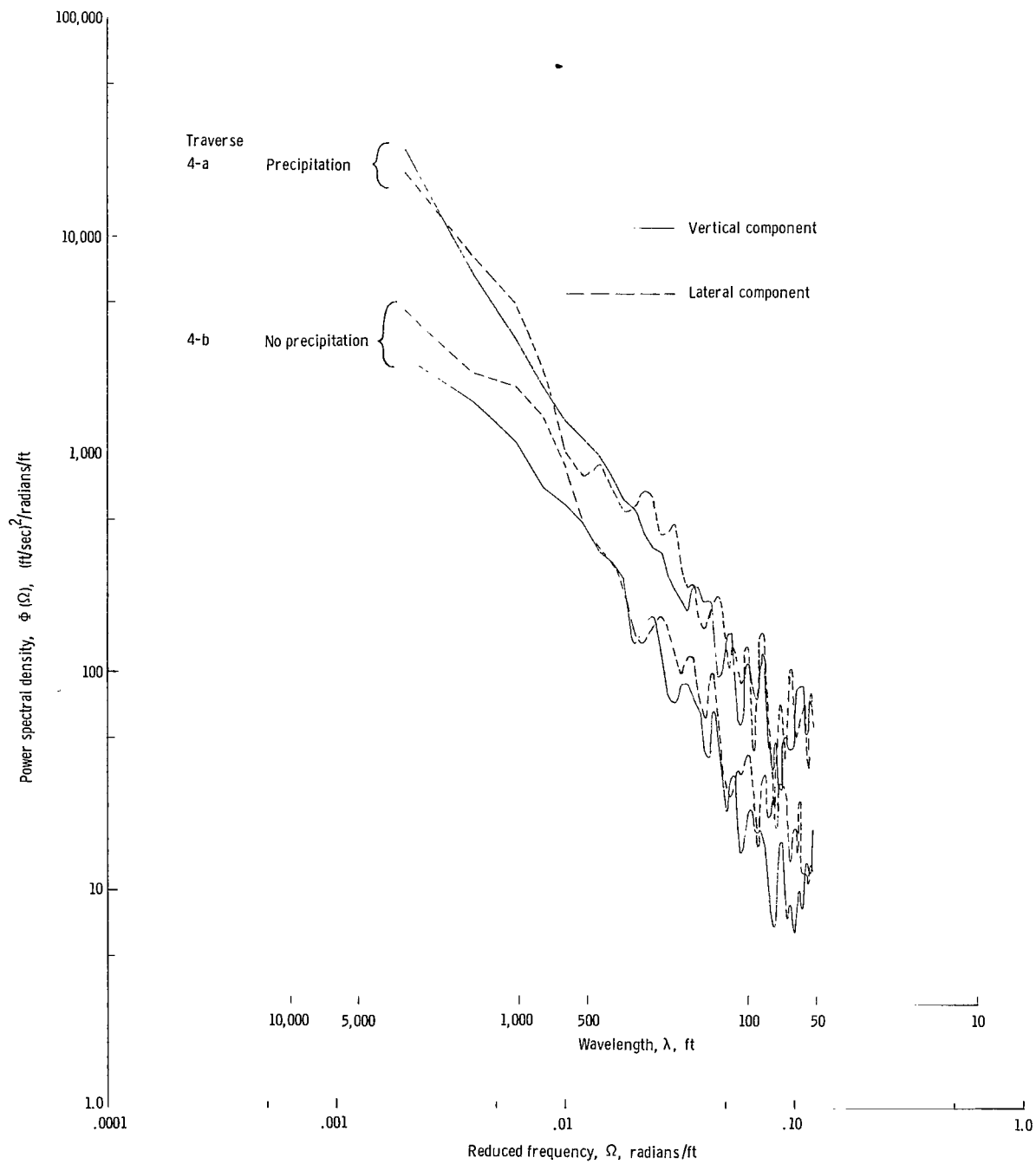
(a) Penetration altitude, 15,000 feet; heading, 040°.

Figure 9.- Comparison of power spectra of turbulence in precipitation and nonprecipitation areas of a developing cumulonimbus cloud.
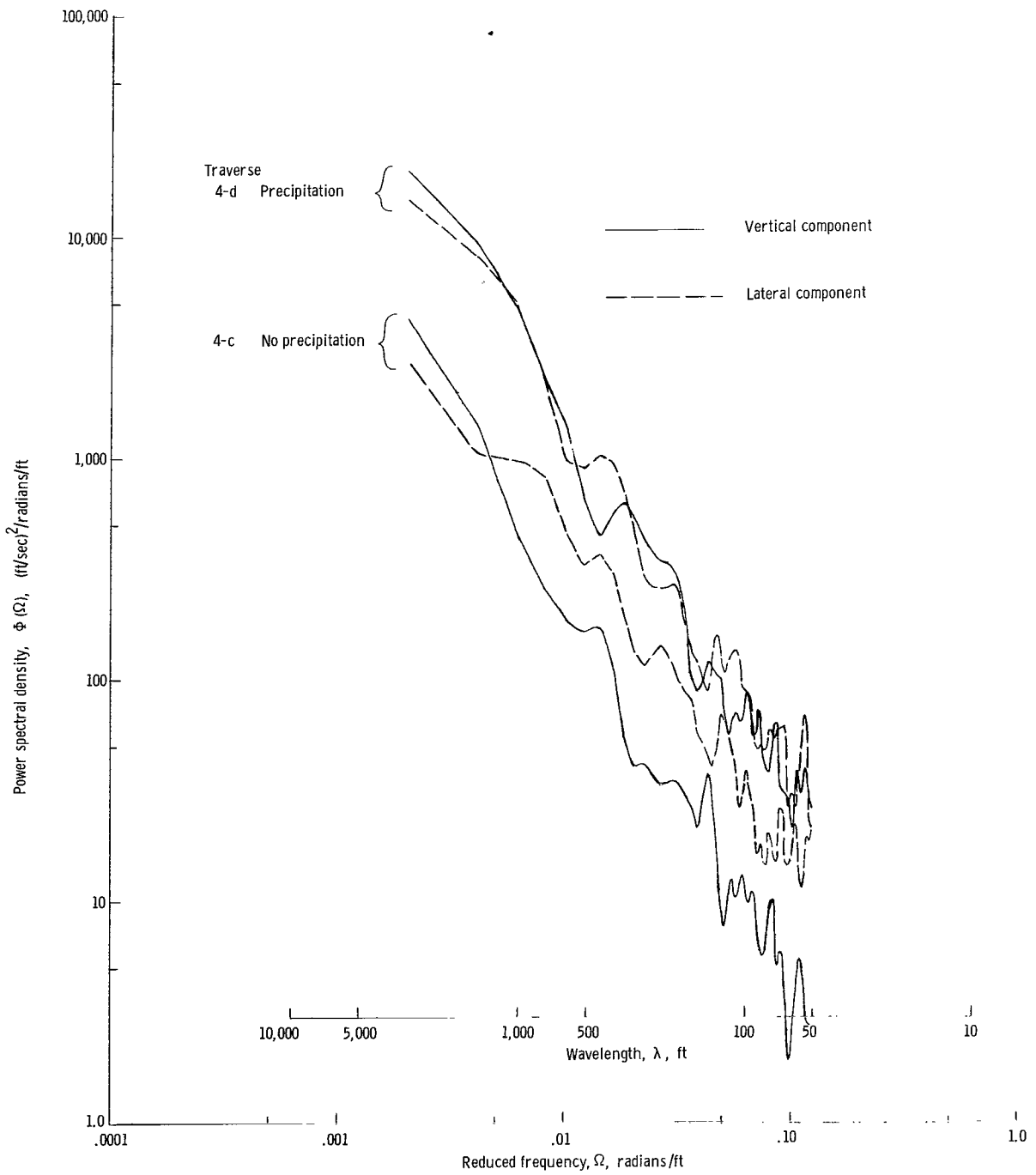
(b) Penetration altitude, 14,200 feet; heading 210° (6 minutes after fig. 9(a) and approximate reciprocal heading).

Figure 9.- Concluded.
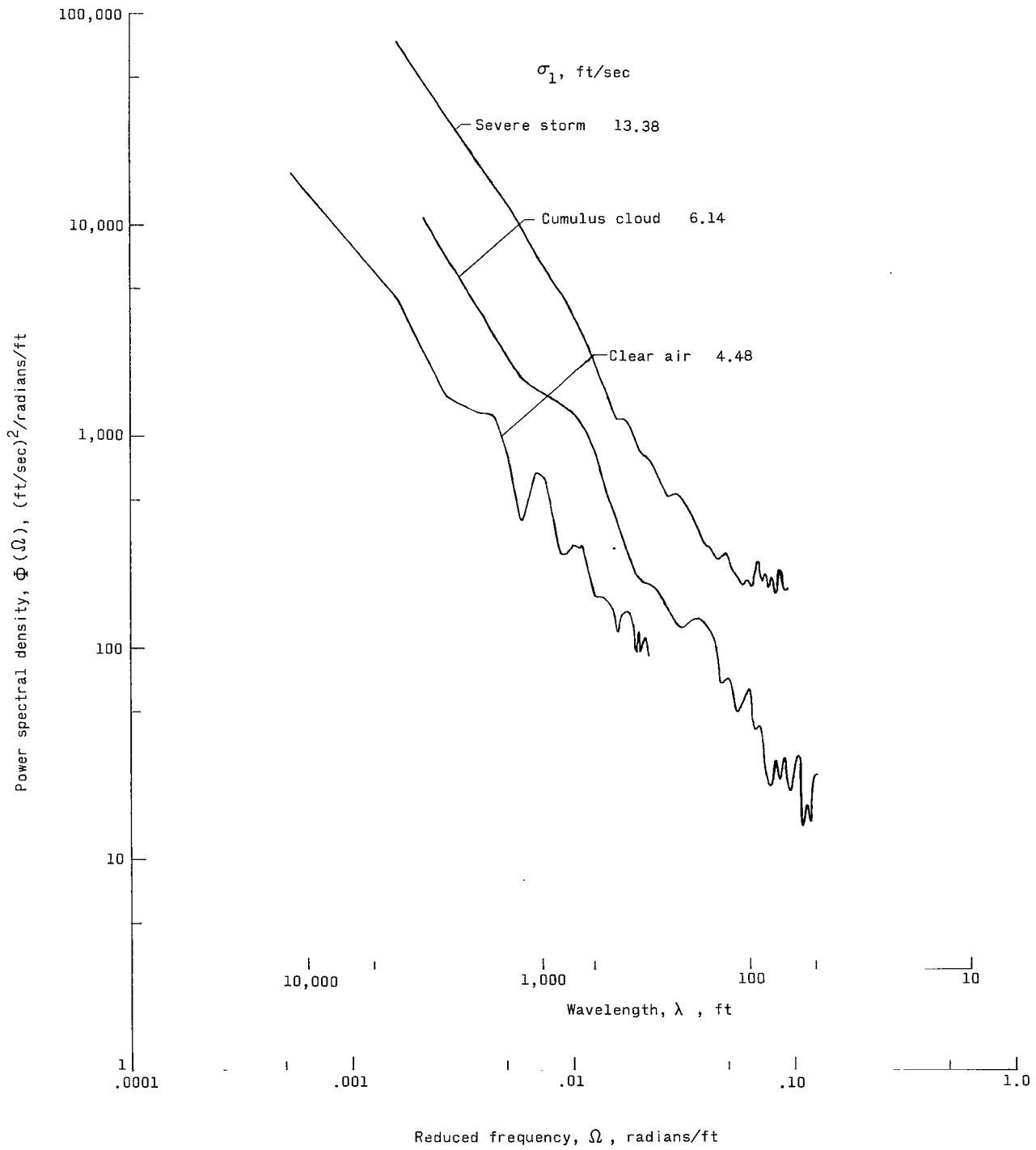
Figure 10.- Typical power spectra of the vertical component of turbulence measured in clear air, cumulus cloud, and severe storm.
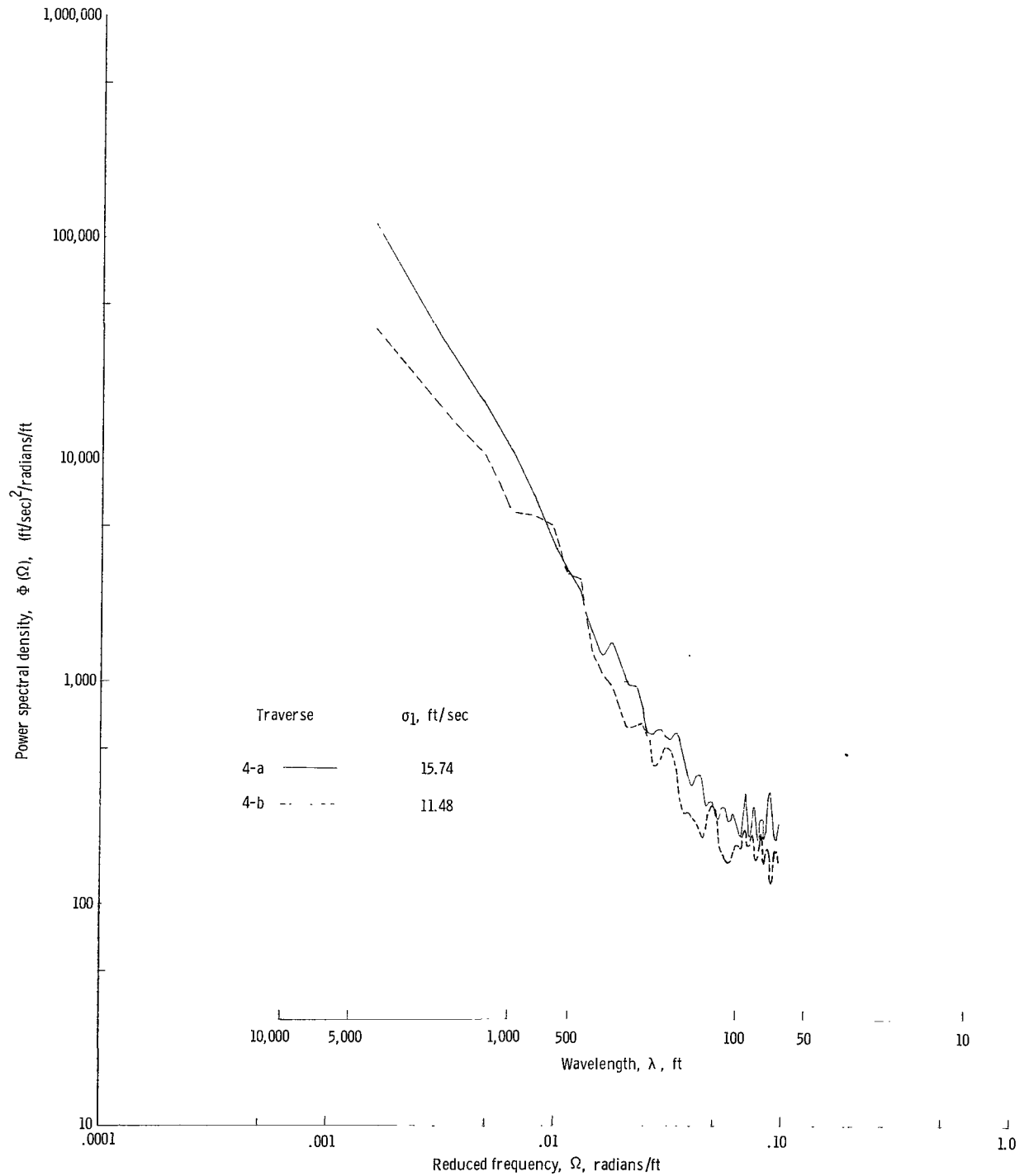
Figure 11.- Comparison of power spectra of the vertical component of turbulence for two parts of severe-storm traverse 4, May 17, 1960.
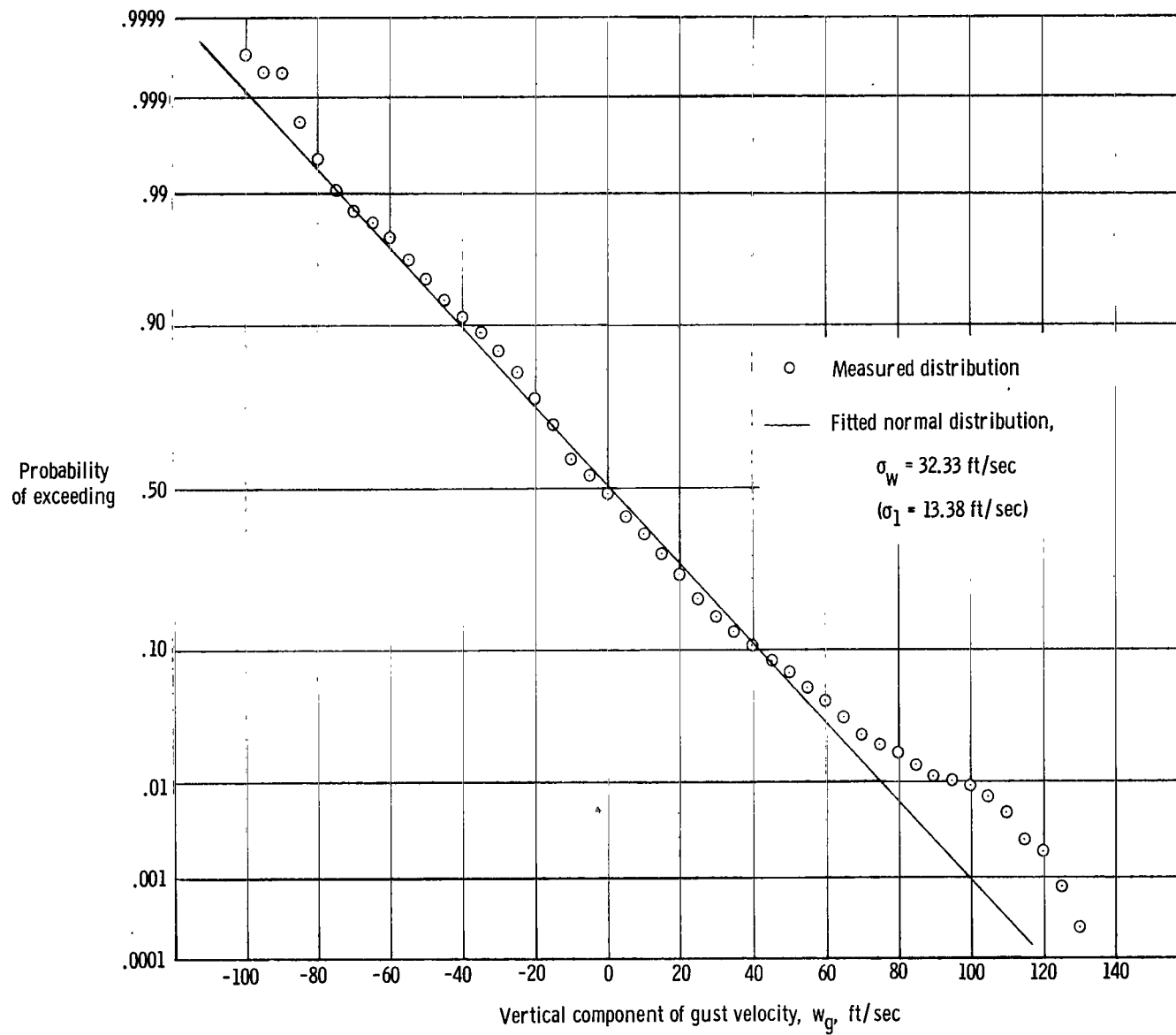
Figure 12.- Probability of equaling or exceeding given values of vertical gust velocity for severe-storm traverse 4, May 17, 1960.
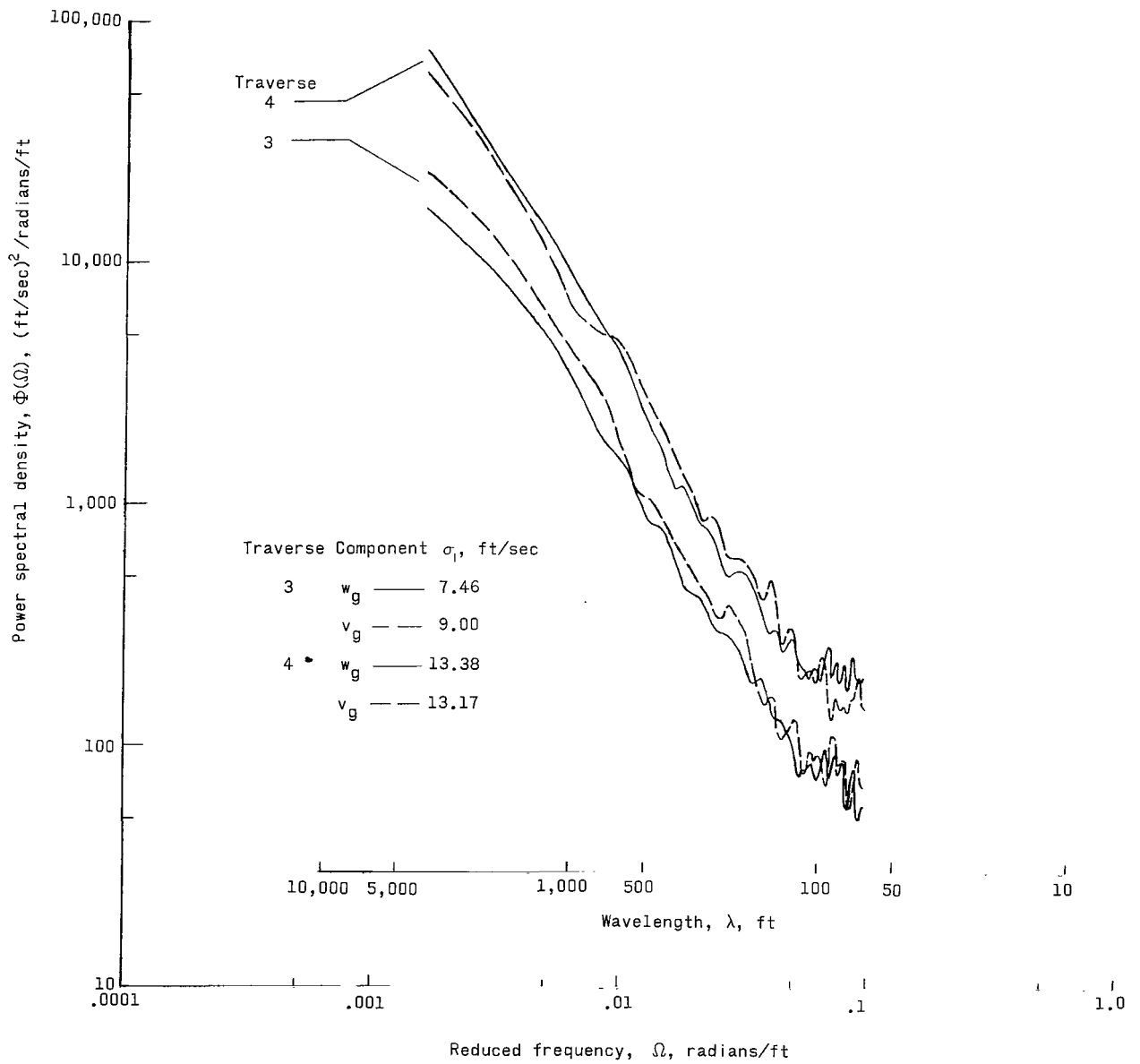
(a) Severe-storm flight of May 17, 1960, 39,000-foot altitude.

Figure 13.- Comparison of the power spectra of the different components of turbulence.
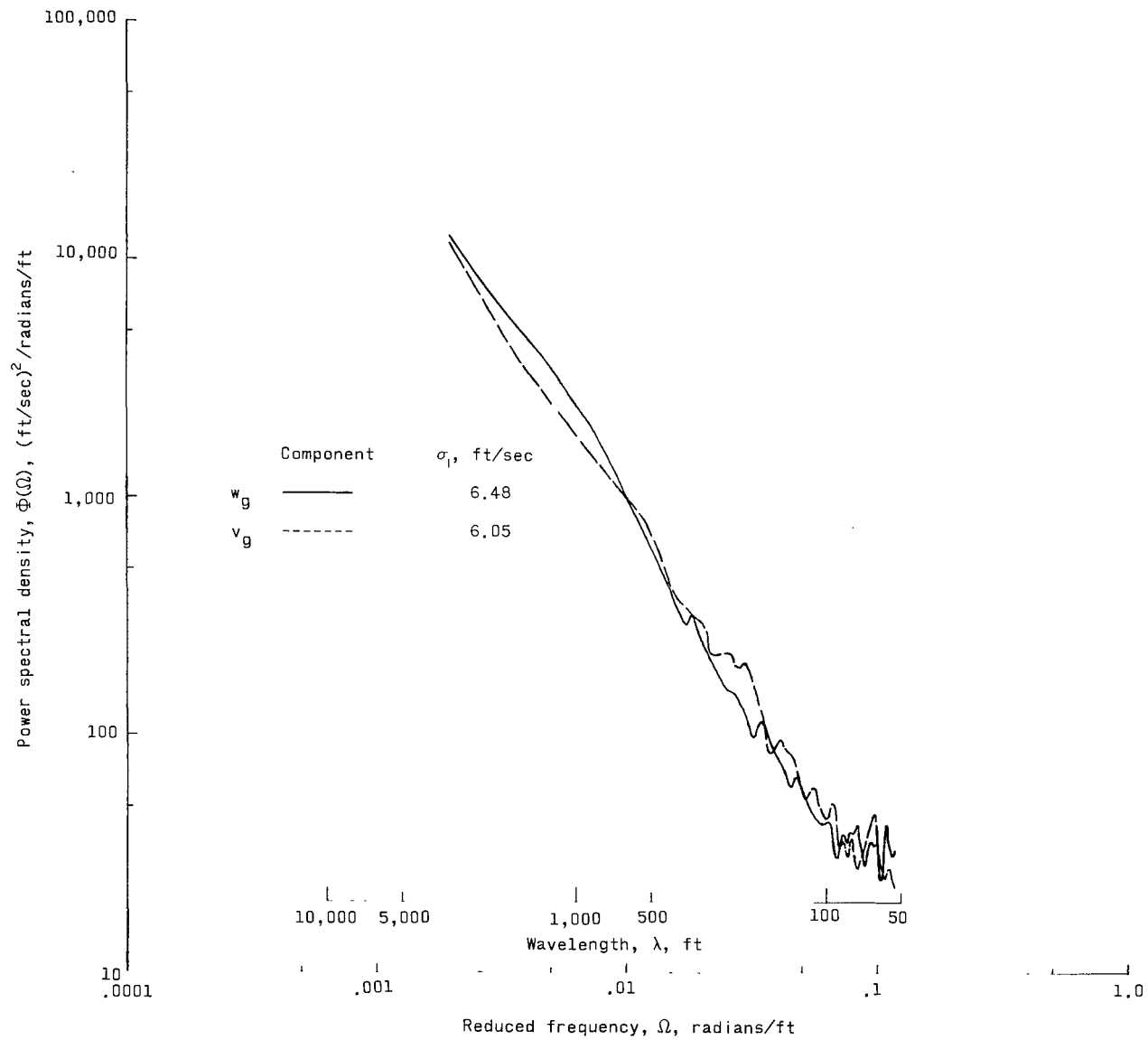
(b) Severe-storm flight of May 4, 1960, traverse 4, 25,000-foot altitude.

Figure 13.- Continued.
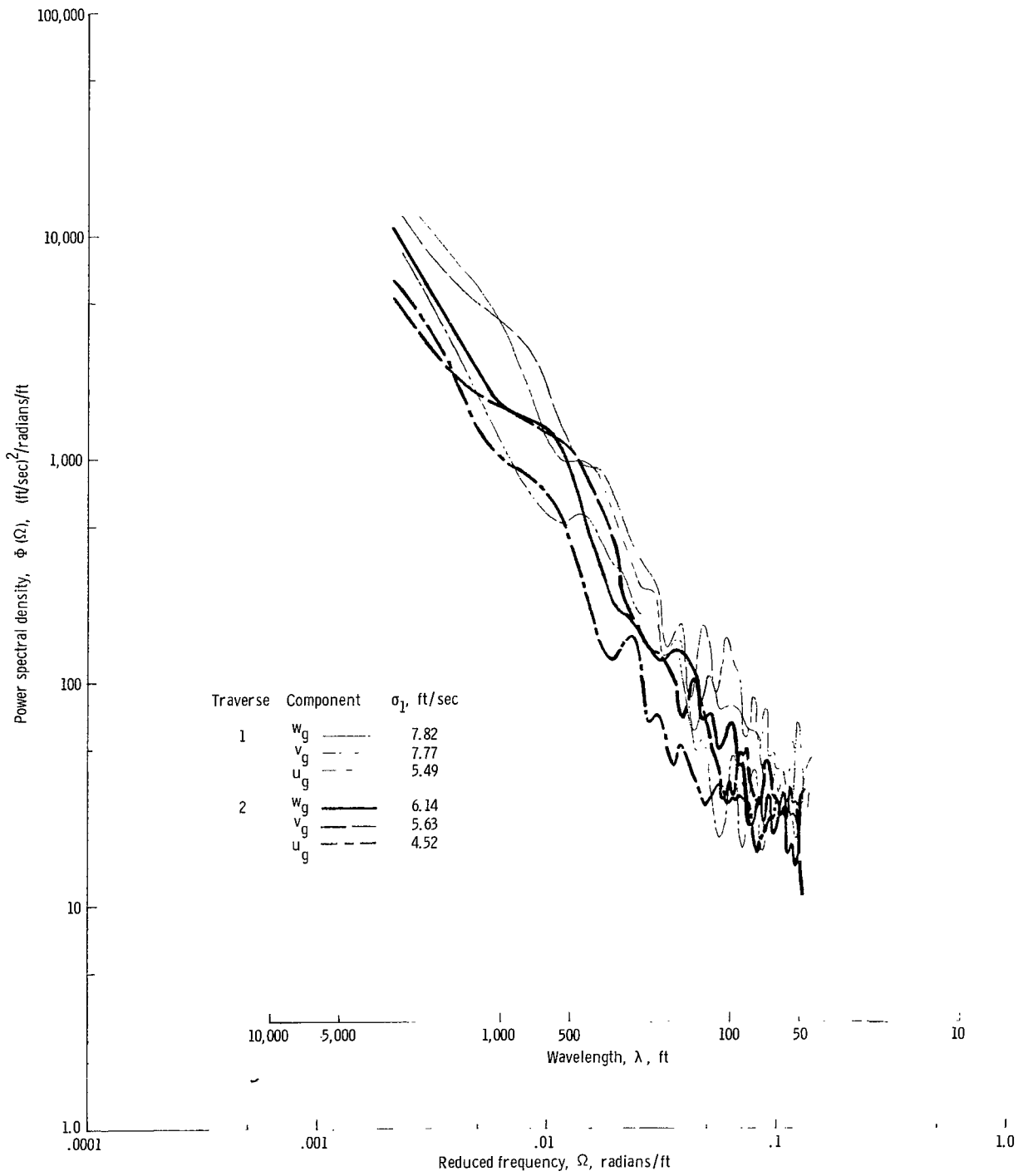
(c) Cumulus-cloud traverses 1 and 2.

Figure 13.- Concluded.
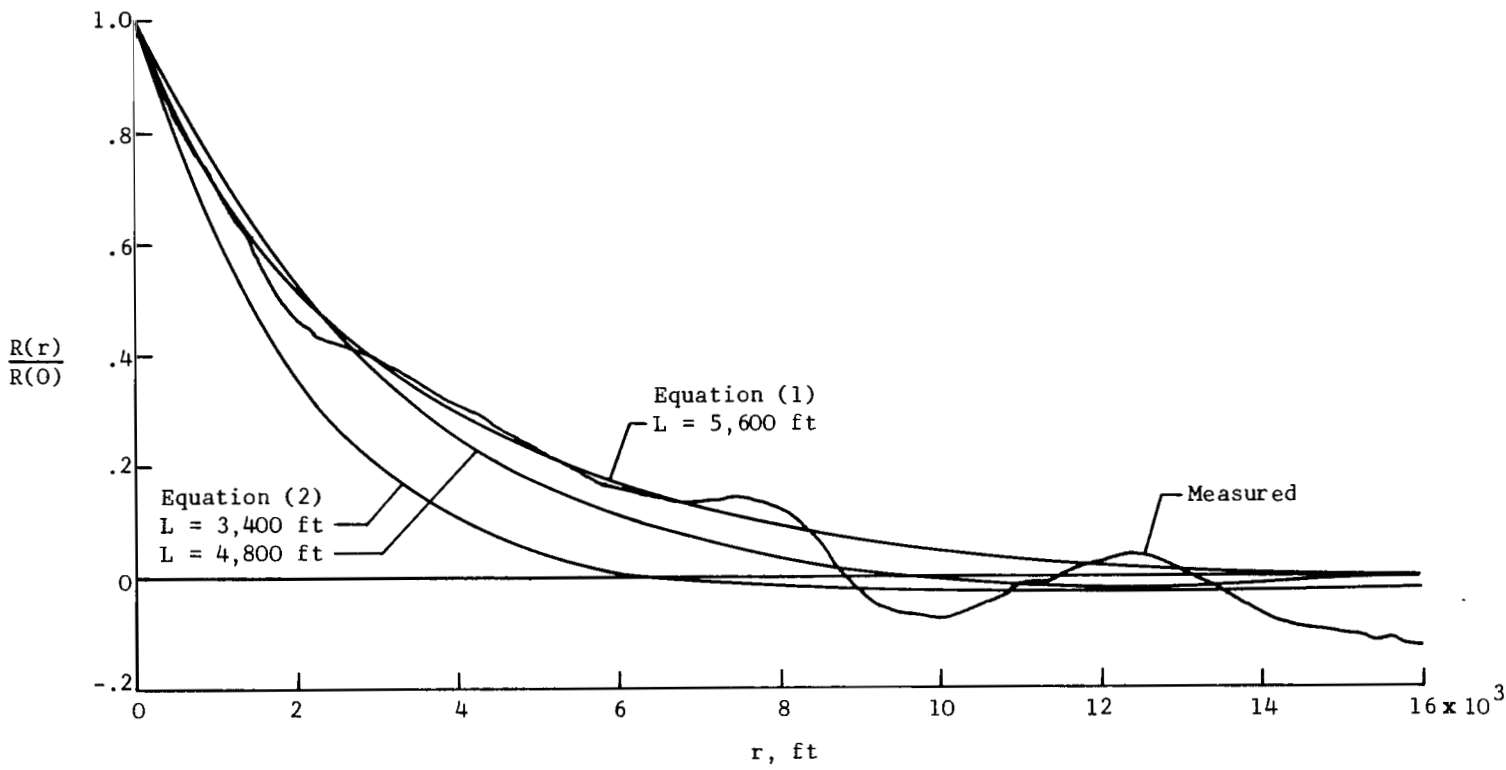
Figure 14.- Measured autocorrelation function and fitted autocorrelation functions corresponding to spectral representations of equations (1) and (2), for severe storm of May 17, 1960. Traverse 4; vertical component.
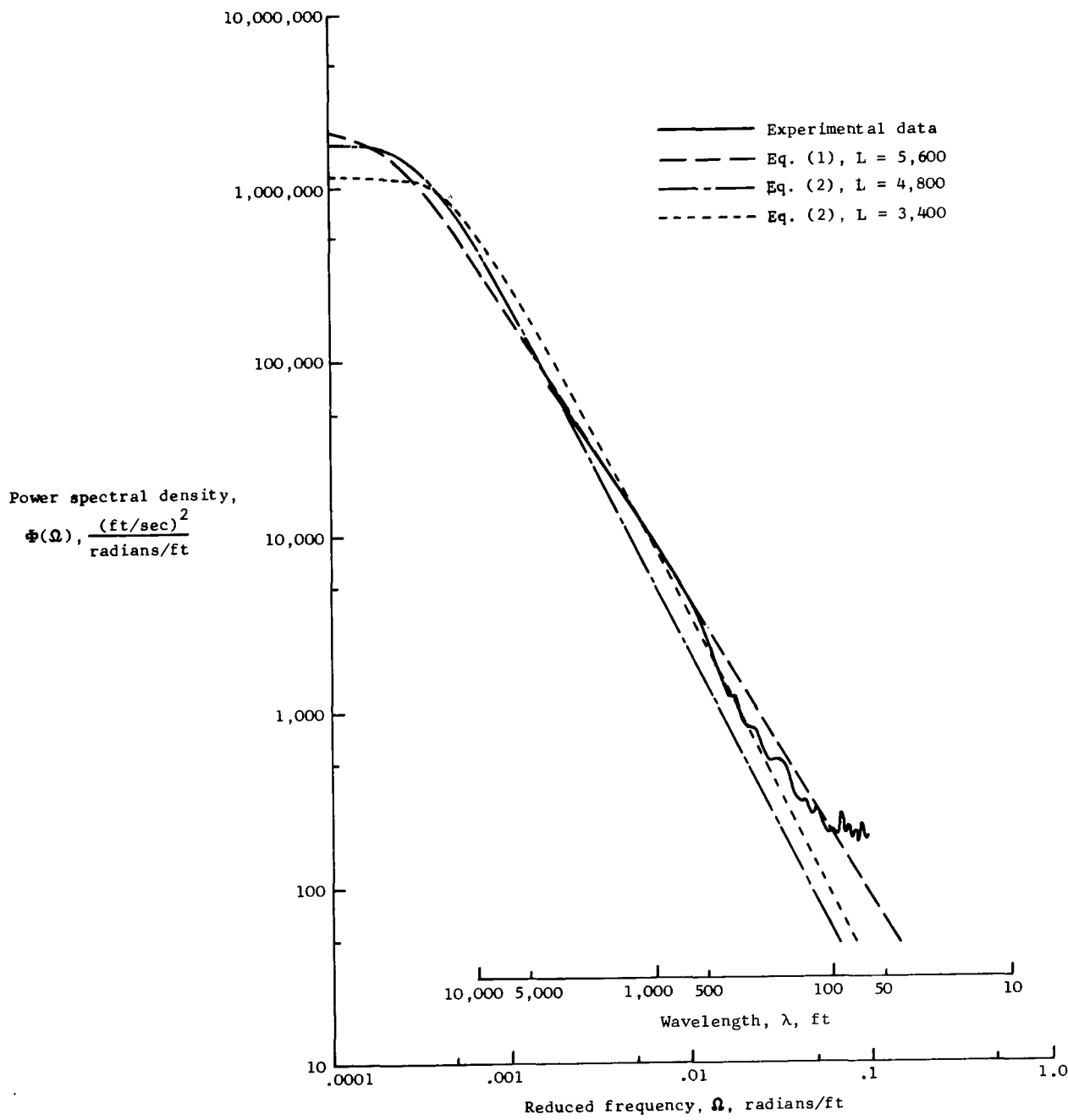
Figure 15.- Measured and fitted spectra for severe storm of May 17, 1960. Traverse 4; vertical component.

NASA SCIENTIFIC AND TECHNICAL PUBLICATIONS

TECHNICAL REPORTS: Scientific and technical information considered important, complete, and a lasting contribution to existing knowledge.

TECHNICAL NOTES: Information less broad in scope but nevertheless of importance as a contribution to existing knowledge.

TECHNICAL MEMORANDUMS: Information receiving limited distribution because of preliminary data, security classification, or other reasons.

CONTRACTOR REPORTS: Technical information generated in connection with a NASA contract or grant and released under NASA auspices.

TECHNICAL TRANSLATIONS: Information published in a foreign language considered to merit NASA distribution in English.

TECHNICAL REPRINTS: Information derived from NASA activities and initially published in the form of journal articles.

SPECIAL PUBLICATIONS: Information derived from or of value to NASA activities but not necessarily reporting the results of individual NASA-programmed scientific efforts. Publications include conference proceedings, monographs, data compilations, handbooks, sourcebooks, and special bibliographies.

Details on the availability of these publications may be obtained from:

SCIENTIFIC AND TECHNICAL INFORMATION DIVISION
NATIONAL AERONAUTICS AND SPACE ADMINISTRATION
Washington, D.C. 20546